Insights into the Reaction Mechanism of the Prolyl-Acyl Carrier Protein Oxidase Involved in Anatoxin-a and Homoanatoxin-a Biosynthesis

Stéphane Mann[‡,], Bérangère Lombard[ǁ], Damarys Loew[ǁ], Annick Méjean[‡,§], and Olivier Ploux[‡,*]

[‡]Chimie ParisTech, ENSCP, Laboratoire Charles Friedel, 11 rue Pierre et Marie Curie, 75231 Paris Cedex 05, France,

CNRS, UMR 7223, 75005 Paris, France

[§]Université Paris Diderot-Paris 7, 75013 Paris, France,

[ǁ]Institut Curie, Centre de Recherche, Laboratory of Proteomic Mass Spectrometry, 26 rue d'Ulm 75248, Paris Cedex 05, France.

[*]To whom correspondence should be addressed. Tel/Fax.: +(33) 1 44 27 67 01. E-mail: olivier-ploux@enscp.fr.

Supporting Information

Figure S1. Alignment of AnaB and human isovaleryl-CoA dehydrogenase (hIVD) sequences. The active site base in hIVD (E254) and the corresponding residue in AnaB (E244) are highlighted in red. A star indicates identity, a colon strong similarity, and a dot weak similarity.

```
hIVD            HSLLPVDDAINGLSEEQRQLRQTMAKFLQEHLAPKAQEIDRSNEFKNLREFWKQLGNLGV 60
AnaB            -----MDFAWN---SQQIQFRKKVIQFAQQSLISDLIKNDKEEIFN--RDAWQKCSEFGV 50
                     :* * *   .:* *:*:.: :* *: * ..  : *:.: *:  *: *:: .::**

hIVD            LGITAPVQYGGSGLGYLEHVLVMEEISRASGAVGLSYG--AHSNLCINQLVRNGNEAQKE 118
AnaB            HGWPIPARYGGQELDILTTAYALQGLGYGCKDNGLIFAMNAHIWACEMPLLTFGTEEQKE 110
                 * . *.:***. *. *  . .:: :. ..   ** :.  **   *   *:  *.* ***

hIVD            KYLPKLISGEYIGALAMSEPNAGSDVVSMKLKAEKKGNHYILNGNKFWITNGPDADVLIV 178
AnaB            KYLPLLCRGGWIASHAATEPQAGSDIYSLKTTAQKDGDKYILNGYKHYVTNGTIADLFII 170
                **** *  * :*.: * :**:****: *:* .*:*.*::***** *.::***. **::*:

hIVD            YAKTDLAAVPASRGITAFIVEKGMPGFSTSKKLDKLGMRGSNTCELIFEDCKIPAANILG 238
AnaB            FATIDPSLG--KEGLTTFMIEKDTPGLILSKPISKMGMRTAEVPELRLENCEVSAANRLG 228
                :*. * :    ..*:*:*::**. **:  ** :.*:*** ::. ** :*:*::.*** **

hIVD            HENKGVYVLMSGLDLERLVLAGGPLGLMQAVLDHTIPYLHVREAFGQKIGHFQLMQGKMA 298
AnaB            EEGTGLAIFNHSMEWERGFILAAAVGTMERLLEQSIRYARSHKQFGQAIGKFQLVANKLV 288
                .*..*: ::  .:: ** .: ...:* *: :*:::* * : :: *** **:***: .*:.

hIVD            DMYTRLMACRQYVYNVAKACDEGHCTAKDCAGVILYSAECATQVALDGIQCFGGNGYIND 358
AnaB            EMKLRLENAKAYLYKVAWMKENKQMALLEASMANLYISEAWVQSCLEAIEIHGAYGYLTN 348
                :*  **  .: *:*:**   :: : :  :.: . ** :*. .* .*:.*: .*. **:.:

hIVD            FPMGRFLRDAKLYEIGAGTSEVRRLVIGRAFNADFH 394
AnaB            TELERELRDAIASKFYSGTSEIQRVVIAKFLGL--- 381
                  : * ****   :: :****::*:**.: :.
```

Figure S2. Polyacrylamide gel electrophoresis in denaturing condition of the purified recombinant wild-type AnaB (WT AnaB) and E244A AnaB. Left: five g of pure fractions were loaded, and the gel was run and stained using coomassie blue. The molecular weight markers (M) were the followings from top to bottom: 66, 45, 36, 29, 24, 20, 14 kDa. Right: the relative migrations of the markers were plotted against their molecular weight on a semilog plot. The data for the following markers: 45, 36, 29, and 24 kDa, were fitted to a logarithmic function using a non-linear regression analysis, which equation is shown below the graph (KaleidaGraph, Synergy Software). AnaB migrated as a 42 kDa rather than as a 46 kDa polypeptide, probably because it was not fully denatured in these conditions or because it was more compact than expected.

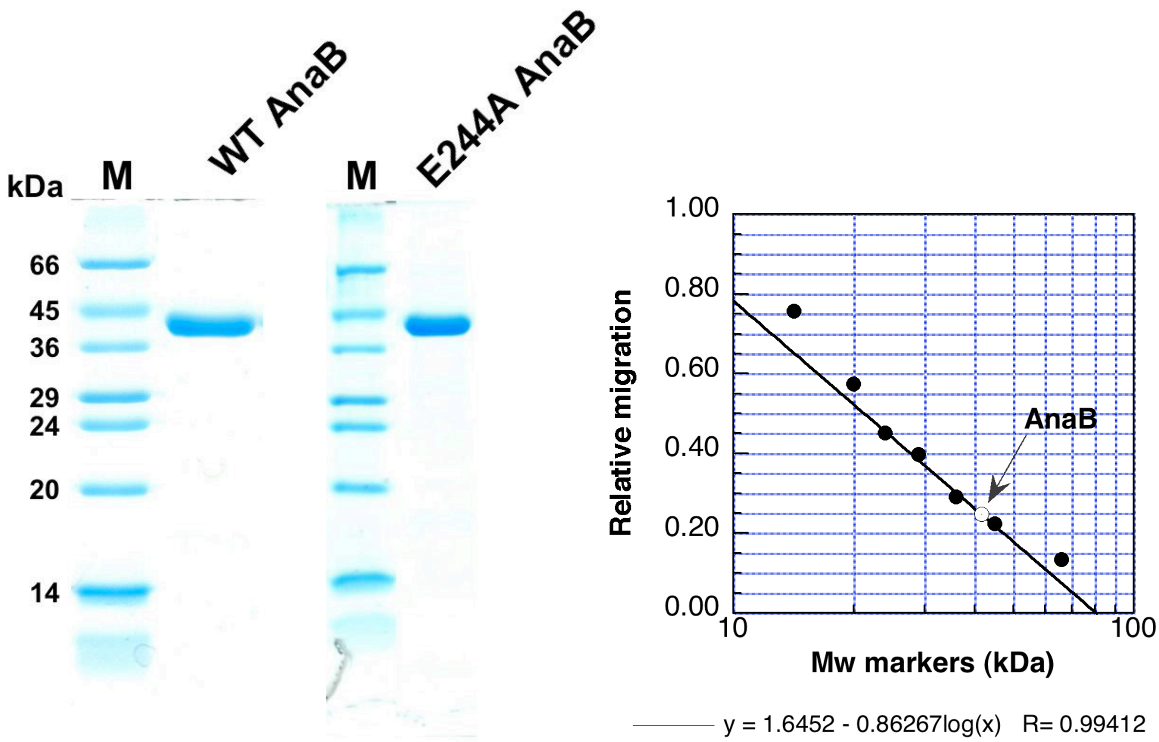

Figure S3-S16. LC-MS/MS analysis of the AnaB-catalyzed oxidation of prolyl-AnaD and of its analogues. The substrates were incubated in the presence of wild-type AnaB, E244A AnaB or in the absence of enzyme, for 5 min at 28 °C. The total ion current chromatograms, the ESI-MS spectra at substrate and product retention times, their deconvoluted mass spectra, and the corresponding MS/MS spectra are presented.

Figure S3. Analysis of the reaction of prolyl-AnaD in the presence of 10 μM wild-type AnaB. A. Analysis of the peak at 15.73 min. The major species is prolyl-AnaD lacking the *N*-terminal Met: observed, 14 246.6 Da, calculated, 14 247.2 Da. Minor species at M + 97 and M + 178 were also observed. B. Analysis of the peak at 16.07 min. The major species is dehydroprolyl-AnaD lacking the *N*-terminal Met: observed, 14 244.8 Da, calculated, 14 245.2 Da. Minor species at M + 97 and M + 178 were also observed.

Figure S4. Analysis of the reaction of prolyl-AnaD in the absence of enzyme. A. Analysis of the peak at 15.55 min. The major species is prolyl-AnaD lacking the *N*-terminal Met: observed, 14 246.4 Da, calculated, 14 247.2 Da. Minor species at M + 97 and M + 178 were also observed. B. Analysis of the shoulder at 16.49 min. Residual intact prolyl-AnaD was observed with a minor species corresponding to prolyl-AnaD lacking the G2-R18 sequence, probably arising from an unexpected proteolytic cleavage at the engineered thrombin site (LVPRGS). No oxidation product was detected. C. The sum of the MS/MS spectra for the charged species (13+, 14+, 15+, 16+, from top to bottom) observed in the region around 16.5 min are presented.

Figure S5. Analysis of the reaction of prolyl-AnaD in the presence of 10 μM E244A AnaB. A. Analysis of the peak at 15.52 min. The major species is prolyl-AnaD lacking the *N*-terminal Met: observed, 14 246.9 Da, calculated, 14 247.2 Da. Minor species at M + 97 and M + 178 were also observed. B. Analysis of the shoulder at 16.78 min. Residual intact prolyl-AnaD was observed. No oxidation product was detected. C. The sum of the MS/MS spectra for the charged species (13+, 14+, 15+, 16+, from top to bottom) observed in the region around 16.2 min are presented.

Figure S6. Analysis of the reaction of [2-^{2}H]-L-prolyl-AnaD in the absence of enzyme. A. Analysis of the peak at 15.62 min. The major species is [2-^{2}H]-L-prolyl-AnaD lacking the *N*-terminal Met: observed, 14 247.2 Da, calculated, 14 248.2 Da. A minor species at M + 178 was also observed. B. Analysis of the shoulder at 17.05 min. Residual intact [2-^{2}H]-L-prolyl-AnaD was observed together with minor species corresponding to prolyl-AnaD lacking the G2-R18 sequence, probably arising from an unexpected proteolytic cleavage at the engineered thrombine site (LVPRGS) and holo-AnaD. No oxidation product was detected.

Figure S7. Analysis of the reaction of [2-^{2}H]-L-prolyl-AnaD in the presence of 10 μM E244A AnaB. A. Analysis of the peak at 16.39 min. The major species is [2-^{2}H]-L-prolyl-AnaD lacking the *N*-terminal Met: observed, 14 247.2 Da, calculated, 14 248.2 Da. Minor species at M + 98 and M + 178 were also observed. B. Analysis of the shoulder at 17.51 min. Residual intact [2-^{2}H]-L-prolyl-AnaD was observed together with minor species corresponding to prolyl-AnaD lacking the G2-R18 sequence, probably arising from an unexpected proteolytic cleavage at the engineered thrombin site (LVPRGS) and holo-AnaD. No oxidation product was detected.

Figure S8. Analysis of the reaction of [2-^{2}H]-L-prolyl-AnaD in the presence of 5 μM wild-type AnaB. A. Analysis of the peak at 16.44 min. The major species is [2-^{2}H]-L-prolyl-AnaD lacking the *N*-terminal Met: observed, 14 247.2 Da, calculated, 14 248.2 Da. Minor species at M + 98 and M + 178 were also observed. The MS/MS spectrum shows the presence of the *m/z* 358 and 359 ions. B. Analysis of the peak at 16.96 min. The major species is dehydroprolyl-AnaD lacking the *N*-terminal Met: observed, 14 245.2 Da, calculated, 14 245.2 Da. Minor species at M + 98 and M + 178 were also observed. The MS/MS spectrum shows a major ion at *m/z* 356.

Figure S9. Analysis of the reaction of [5,5-$^2H_2$]-L-prolyl-AnaD in the presence of 10 μM wild-type AnaB. A. Analysis of the peak at 16.68 min. The major species is [5,5-$^2H_2$]-L-prolyl-AnaD lacking the *N*-terminal Met: observed, 14 248.3 Da, calculated, 14 249.2 Da. Minor species at M + 99 and M + 178 were also observed. B. Analysis of the peak at 17.03 min. The major species is [5-^{2}H]-dehydroprolyl-AnaD lacking the *N*-terminal Met: observed, 14 245.4 Da, calculated, 14 246.2 Da. Minor species at M + 99 and M + 178 were also observed.

Figure S10. Analysis of the reaction of (5*S*)-[5-^{2}H]-L-prolyl-AnaD in the presence of 10 μM wild-type AnaB. A. Analysis of the peak at 16.40 min. The major species is (5*S*)-[5-^{2}H]-L-prolyl-AnaD lacking the *N*-terminal Met: observed, 14 247.1 Da, calculated, 14 248.2 Da. Minor species at M + 98 and M + 178 were also observed. B. Analysis of the peak at 16.81 min. The major species is [5-^{2}H]-dehydroprolyl-AnaD lacking the *N*-terminal Met: observed, 14 245.6 Da, calculated, 14 246.2 Da. Minor species at M + 98 and M + 178 were also observed.

Figure S11. Analysis of the reaction of [2,3,3,4,4,5,5-$^2H_7$]-L-prolyl-AnaD in the absence of enzyme. A. Analysis of the peak at 16.40 min. The major species is [2,3,3,4,4,5,5-$^2H_7$]-L-prolyl-AnaD lacking the *N*-terminal Met: observed, 14 253.5 Da, calculated, 14 254.2 Da. Minor species at M + 104 and M + 178 were also observed. B. Analysis of the peak at 17.49 min. Residual [2,3,3,4,4,5,5-$^2H_7$]-L-prolyl-AnaD was observed together with degraded species: holo-AnaD (14 150.1 Da) and thrombin digested species (12 503.4 Da). No oxidation product was observed.

Figure S12. Analysis of the reaction of [2,3,3,4,4,5,5-$^2H_7$]-L-prolyl-AnaD in the presence of 10 μM E244A AnaB. A. Analysis of the peak at 16.23 min. The major species is [2,3,3,4,4,5,5-$^2H_7$]-L-prolyl-AnaD lacking the *N*-terminal Met: observed, 14 253.6 Da, calculated, 14 254.2 Da. Minor species at M + 104 and M + 178 were also observed. B. Analysis of the peak at 17.40 min. Residual [2,3,3,4,4,5,5-$^2H_7$]-L-prolyl-AnaD was observed together with degradaded species: holo-AnaD (14 150.1 Da) and thrombin digested species (12 503.4 Da). No oxidation product was observed. C. The sum of the MS/MS spectra for the charged species (13+, 14+, 15+, 16+, from top to bottom) observed in the region around 17.5 min are presented. Enlargements of the spectra are shown on the right hand side.

Figure S13. Analysis of the reaction of [2,3,3,4,4,5,5-$^2H_7$]-L-prolyl-AnaD in the presence of 10 μM wild-type AnaB. A. Analysis of the peak at 15.90 min. The major species is [3,3,4,4,5,5-$^2H_6$]-L-prolyl-AnaD lacking the *N*-terminal Met: observed, 14 252.5 Da, calculated, 14 253.2 Da. Minor species at M + 104 and M + 178 were also observed. B. Analysis of the peak at 16.66 min. The major species is deuterium labeled dehydroprolyl-AnaD lacking the *N*-terminal Met: observed, 14 250.0 Da. This species corresponded to M + 5 (labeled with five deuteriums). A minor species at and M + 178 was also observed. C. The sum of the MS/MS spectra for the charged species (13+, 14+, 15+, 16+, from top to bottom) observed in the region around 16.5 min are presented. Enlargements of the spectra are shown on the right hand side.

Figure S14. Analysis of the reaction of 3,4-dehydro-L-prolyl-AnaD in the presence of 10 μM wild-type AnaB. A. Analysis of the peak at 16.10 min. The major species is 3,4-dehydro-L-prolyl-AnaD lacking the *N*-terminal Met: observed, 14 244.7 Da, calculated, 14 244.8 Da. Minor species at M + 95 and M + 178 were also observed. B. Analysis of the peak at 16.81 min. The major species is pyrrole-2-carboxyl-AnaD lacking the *N*-terminal Met: observed, 14 243.1 Da, calculated 14 243.8 Da. Minor species at M – 94 (holo-AnaD), M + 95 and M + 178 and residual 3,4-dehydro-L-prolyl-AnaD were also observed.

Figure S15. Analysis of the reaction of (4*S*)-4-fluoro-L-prolyl-AnaD in the presence of 10 μM wild-type AnaB. A. Analysis of the peak at 15.79 min. The major species is (4*S*)-4-fluoro-L-prolyl-AnaD lacking the *N*-terminal Met: observed, 14 264.4 Da, calculated, 14 265.2 Da. Minor species at M + 115 and M + 178 were also observed. B. Analysis of the peak at 16.92 min. The pyrrole-2-carboxyl-AnaD lacking the *N*-terminal Met was observed (observed 14 242.7 Da, calculated 14 243.8 Da) together with (4*S*)-4-fluoro-L-prolyl-AnaD and some thrombin digested species (12 514 Da). C. The sum of the MS/MS spectra for the charged species (13+, 14+, 15+, from top to bottom) observed in the region around 17.2 min are presented. Enlargements of the spectra are shown on the right hand side.

Figure S16. Analysis of the reaction of (4*R*)-4-fluoro-L-prolyl-AnaD in the presence of 10 μM wild-type AnaB. A. Analysis of the peak at 15.97 min. The major species is (4*R*)-4-fluoro-L-prolyl-AnaD lacking the *N*-terminal Met: observed, 14 264.6 Da, calculated, 14 265.2 Da. Minor species at M + 115 and M + 178 were also observed. B. Analysis of the peak at 16.87 min. The major species is pyrrole-2-carboxyl-AnaD lacking the *N*-terminal Met: observed 14 242.5 Da, calculated 14 243.8 Da. Minor species at M + 115 and M + 178 were also observed.

Figure S3A.

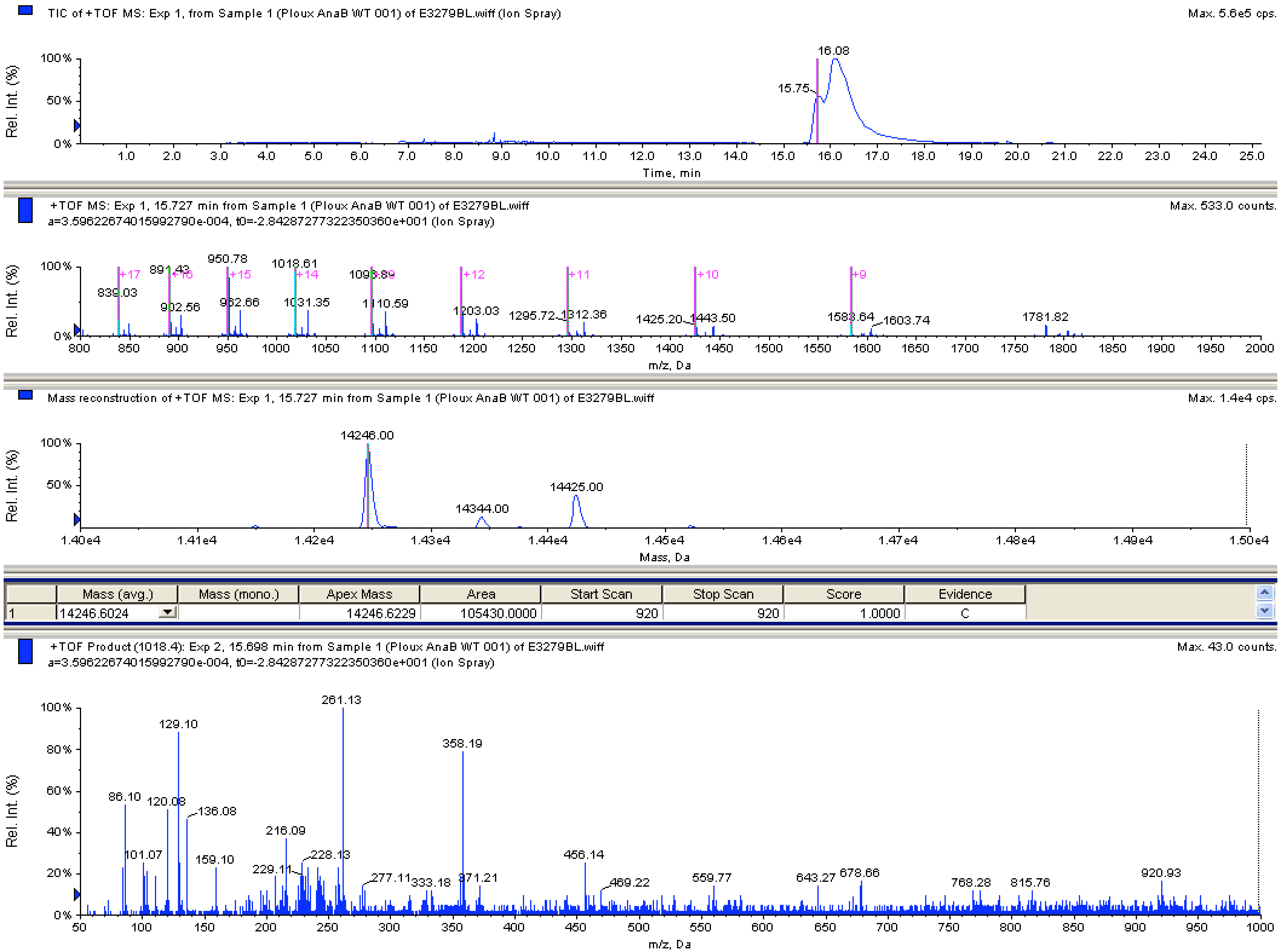
TIC of +TOF MS: Exp 1, from Sample 1 (Ploux AnaB WT 001) of E3279BL.wiff (Ion Spray)
Max. 5.6e5 cps.
Rel. Int. (%)
16.08
15.75
Time, min
+TOF MS: Exp 1, 15.727 min from Sample 1 (Ploux AnaB WT 001) of E3279BL.wiff
a=3.59622674015992790e-004, t0=-2.84287277322350360e+001 (Ion Spray)
Max. 533.0 counts.
839.03
891.43
902.56
950.78
952.66
1018.61
1031.35
1096.89
1110.59
1203.03
1295.72
1312.36
1425.20
1443.50
1583.64
1603.74
1781.82
+17
+16
+15
+14
+12
+11
+10
+9
m/z, Da
Mass reconstruction of +TOF MS: Exp 1, 15.727 min from Sample 1 (Ploux AnaB WT 001) of E3279BL.wiff
Max. 1.4e4 cps.
14246.00
14344.00
14425.00
Mass, Da
Mass (avg.) | Mass (mono.) | Apex Mass | Area | Start Scan | Stop Scan | Score | Evidence
1 | 14246.6024 | | 14246.6229 | 105430.0000 | 920 | 920 | 1.0000 | C
+TOF Product (1018.4): Exp 2, 15.698 min from Sample 1 (Ploux AnaB WT 001) of E3279BL.wiff
a=3.59622674015992790e-004, t0=-2.84287277322350360e+001 (Ion Spray)
Max. 43.0 counts.
261.13
129.10
358.19
86.10
120.08
136.08
216.09
101.07
159.10
228.13
229.11
277.11
333.18
371.21
456.14
469.22
559.77
643.27
678.66
768.28
815.76
920.93
m/z, Da

Figure S3B.

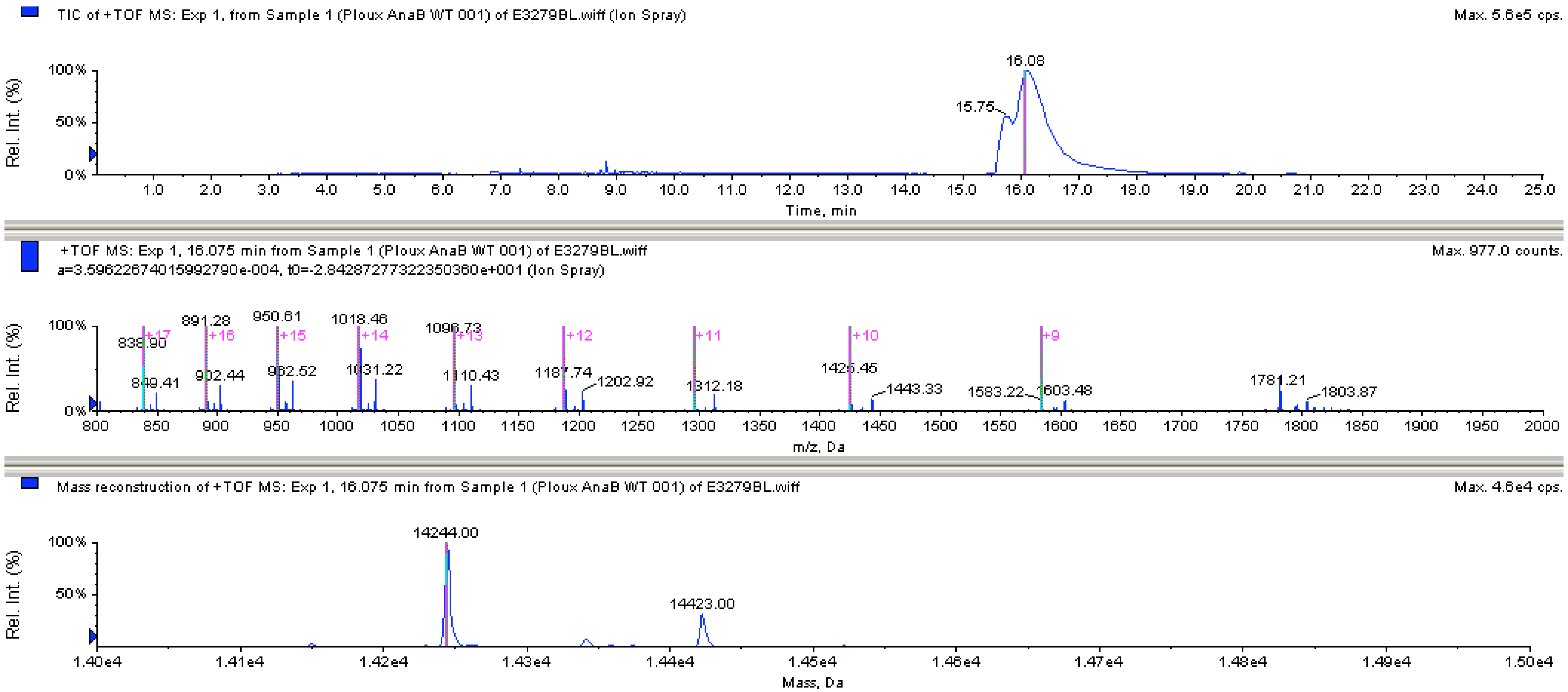

	Mass (avg.)	Mass (mono.)	Apex Mass	Area	Start Scan	Stop Scan	Score	Evidence
1	14244.7971		14244.6673	263286.8652	928	928	1.0000	C

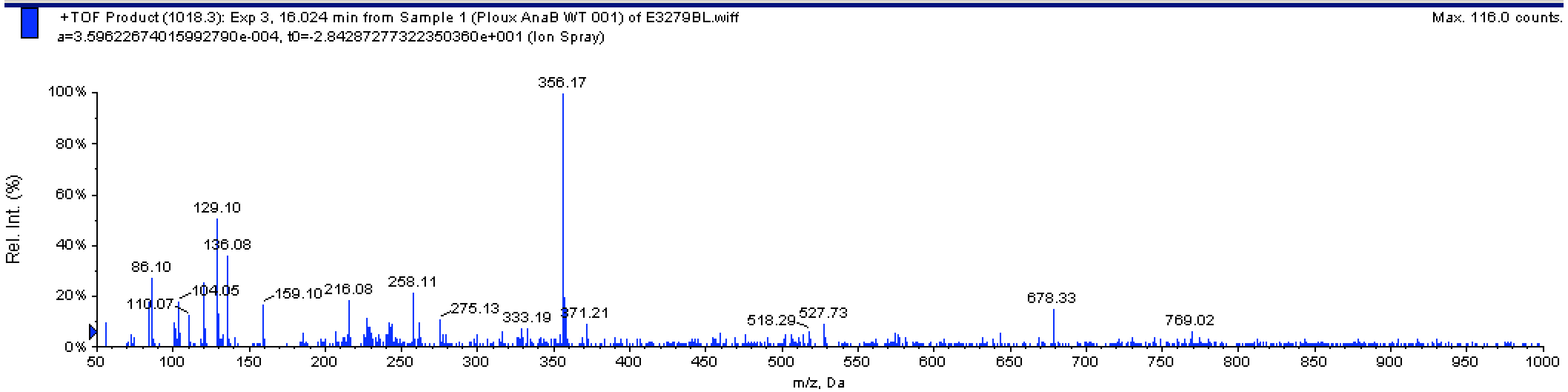

Figure S4A.

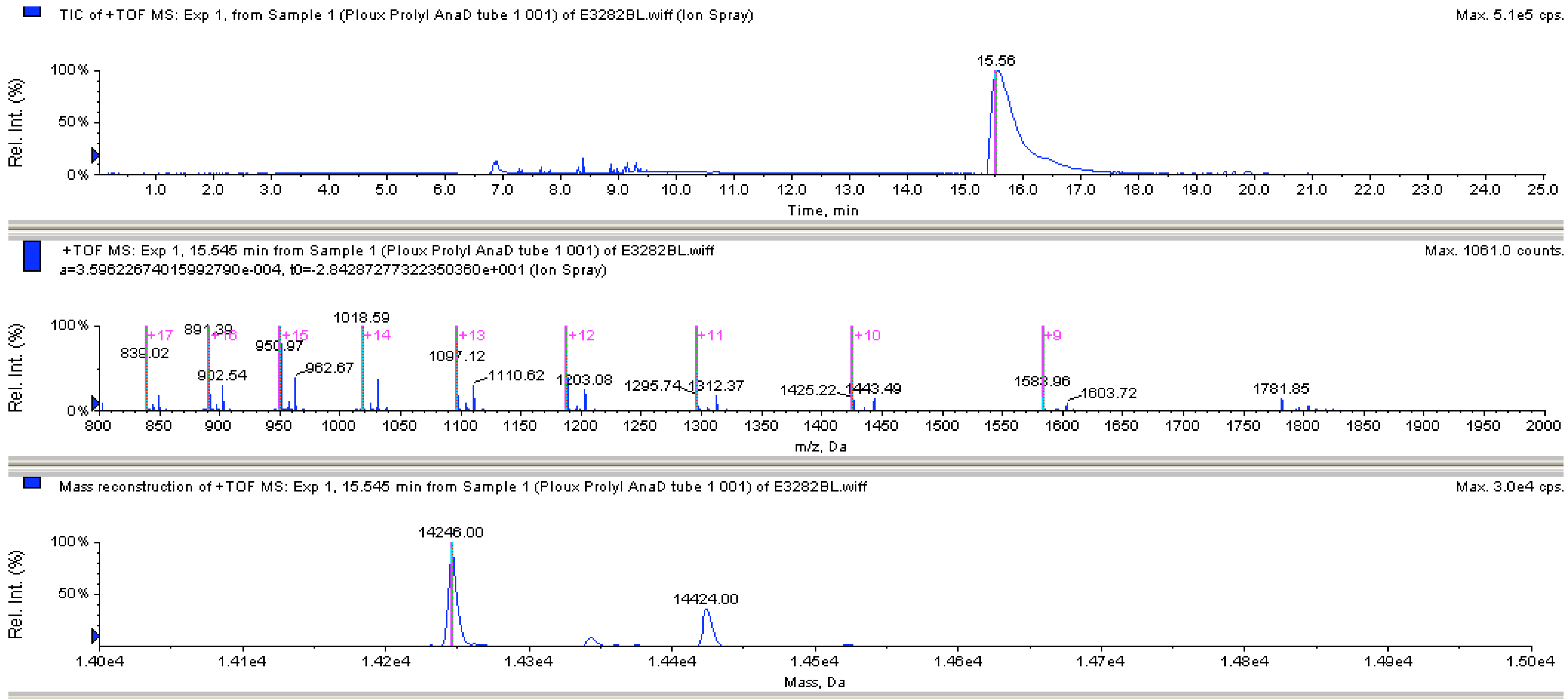

	Mass (avg.)	Mass (mono.)	Apex Mass	Area	Start Scan	Stop Scan	Score	Evidence
1	14246.4271		14246.3592	211592.0000	911	911	1.0000	C

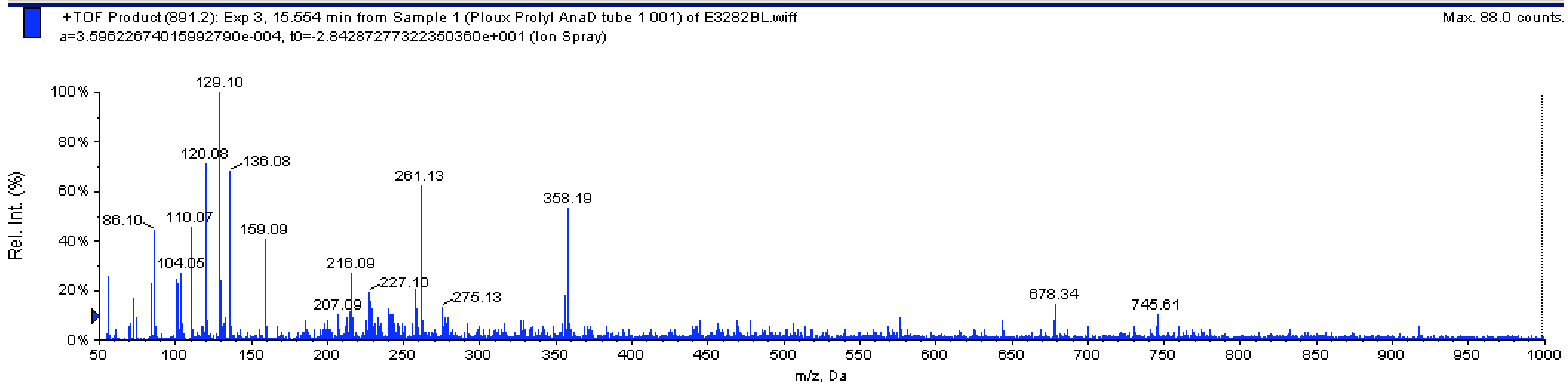

Figure S4B.

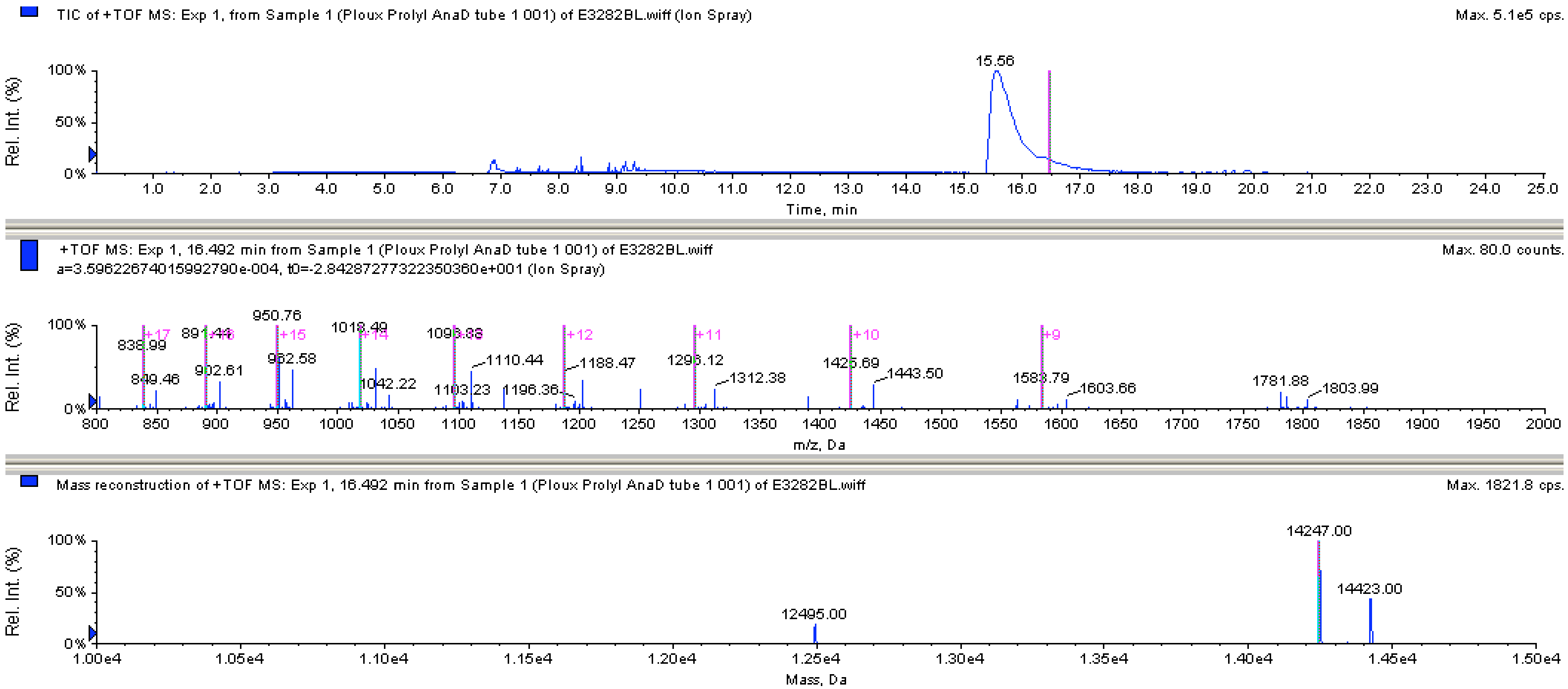

	Mass (avg.)	Mass (mono.)	Apex Mass	Area	Start Scan	Stop Scan	Score	Evidence
1	14246.3740		14246.4398	14479.0000	927	927	1.0000	C

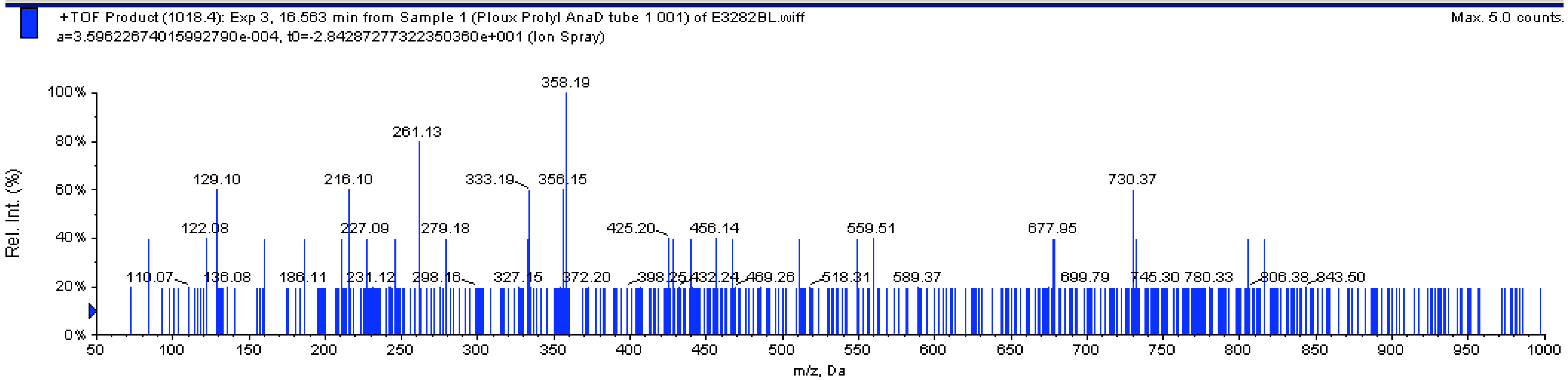

Figure S4C.

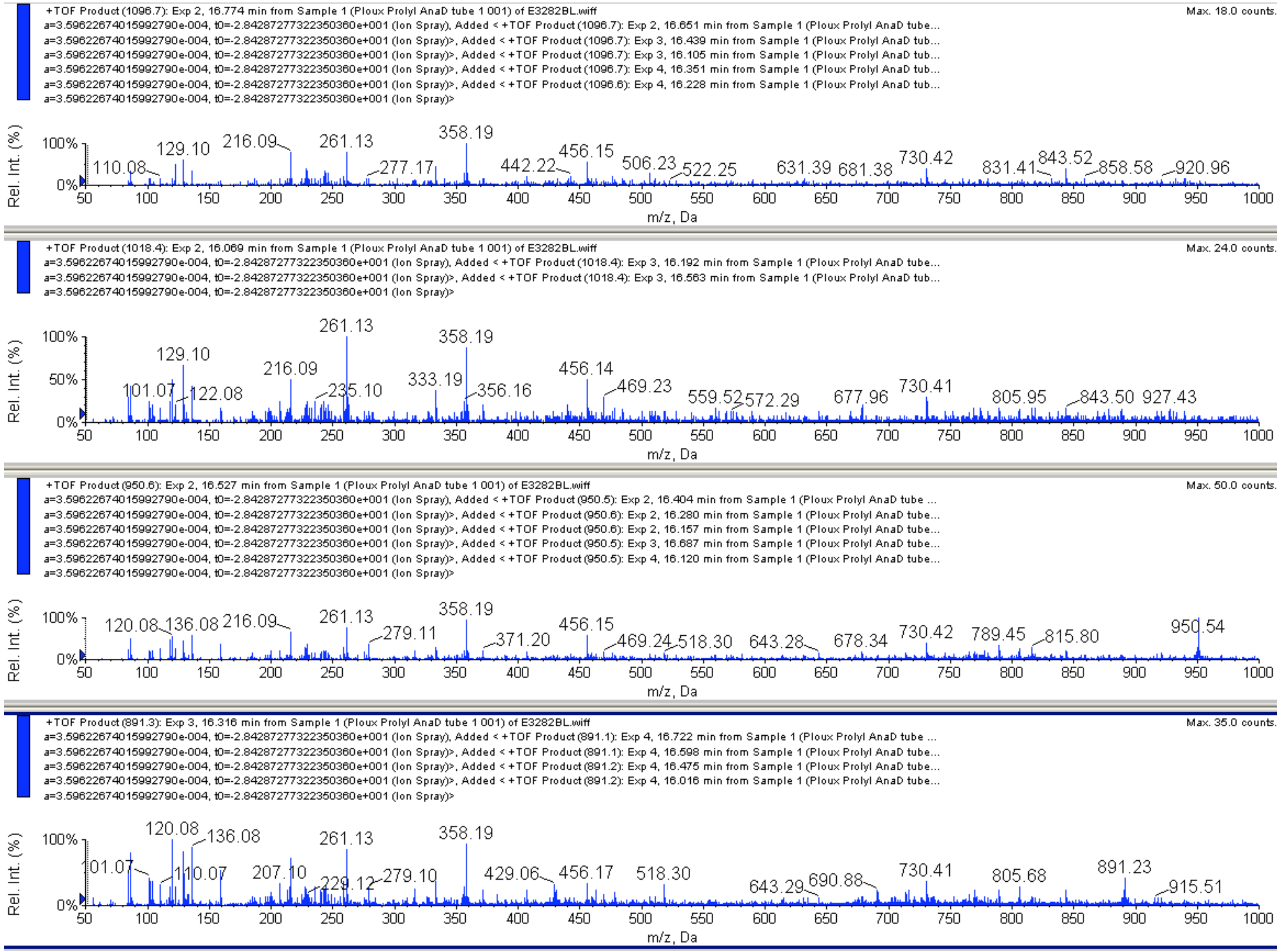
+TOF Product (1096.7): Exp 2, 16.774 min from Sample 1 (Ploux Prolyl AnaD tube 1 001) of E3282BL.wiff
Max. 18.0 counts.
Rel. Int. (%)
100%
0%
110.08
129.10
216.09
261.13
277.17
358.19
442.22
456.15
506.23
522.25
631.39
681.38
730.42
831.41
843.52
858.58
920.96
m/z, Da
+TOF Product (1018.4): Exp 2, 16.069 min from Sample 1 (Ploux Prolyl AnaD tube 1 001) of E3282BL.wiff
Max. 24.0 counts.
101.07
122.08
129.10
216.09
235.10
261.13
333.19
356.16
358.19
456.14
469.23
559.52
572.29
677.96
730.41
805.95
843.50
927.43
+TOF Product (950.6): Exp 2, 16.527 min from Sample 1 (Ploux Prolyl AnaD tube 1 001) of E3282BL.wiff
Max. 50.0 counts.
120.08
136.08
216.09
261.13
279.11
358.19
371.20
456.15
469.24
518.30
643.28
678.34
730.42
789.45
815.80
950.54
+TOF Product (891.3): Exp 3, 16.316 min from Sample 1 (Ploux Prolyl AnaD tube 1 001) of E3282BL.wiff
Max. 35.0 counts.
101.07
110.07
120.08
136.08
207.10
229.12
261.13
279.10
358.19
429.06
456.17
518.30
643.29
690.88
730.41
805.68
891.23
915.51

Figure S5A.

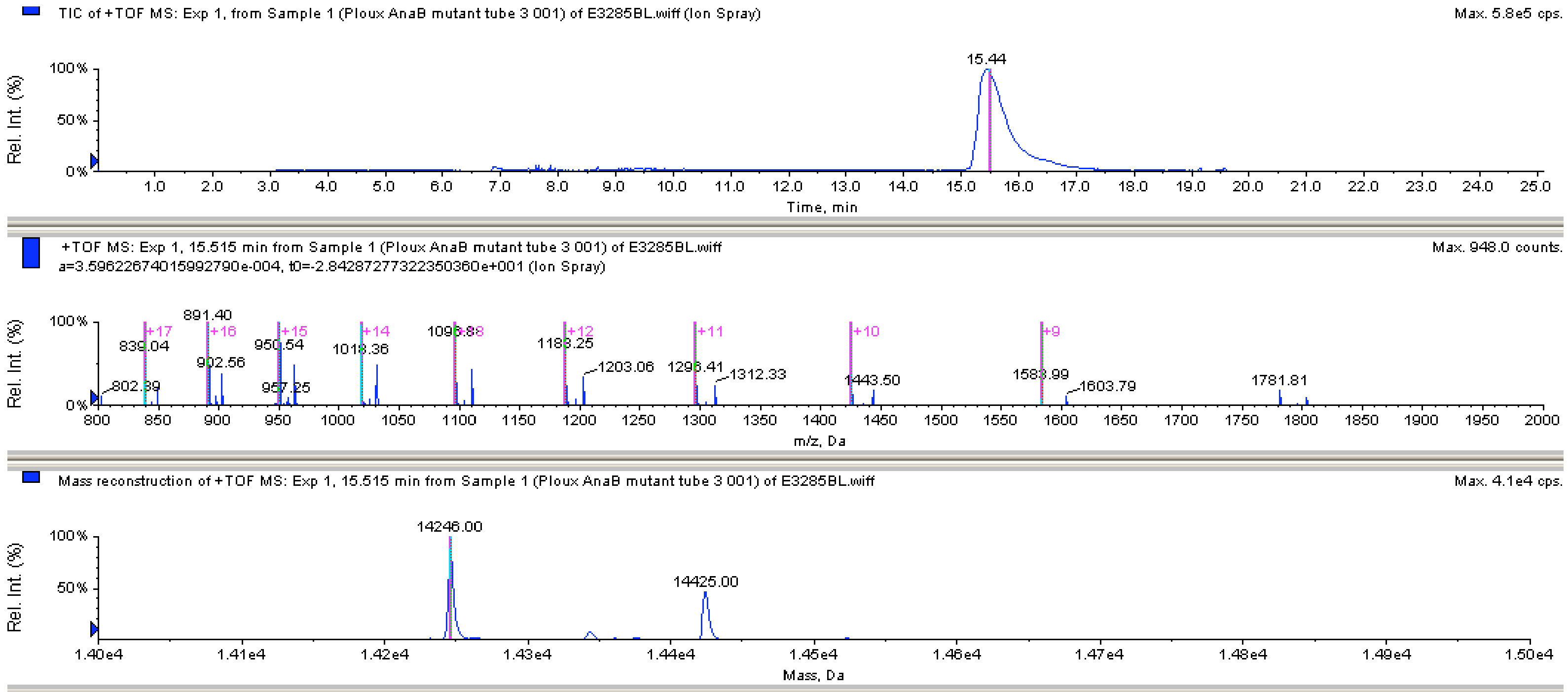

	Mass (avg.)	Mass (mono.)	Apex Mass	Area	Start Scan	Stop Scan	Score	Evidence
1	14246.8712		14246.7840	243406.2324	903	903	1.0000	C

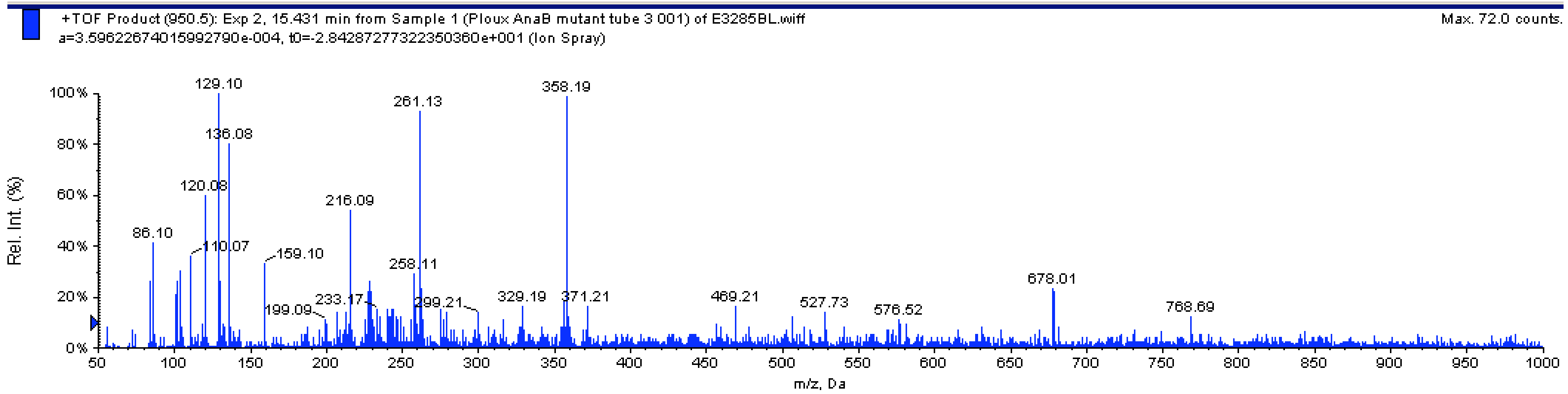

Figure S5B.

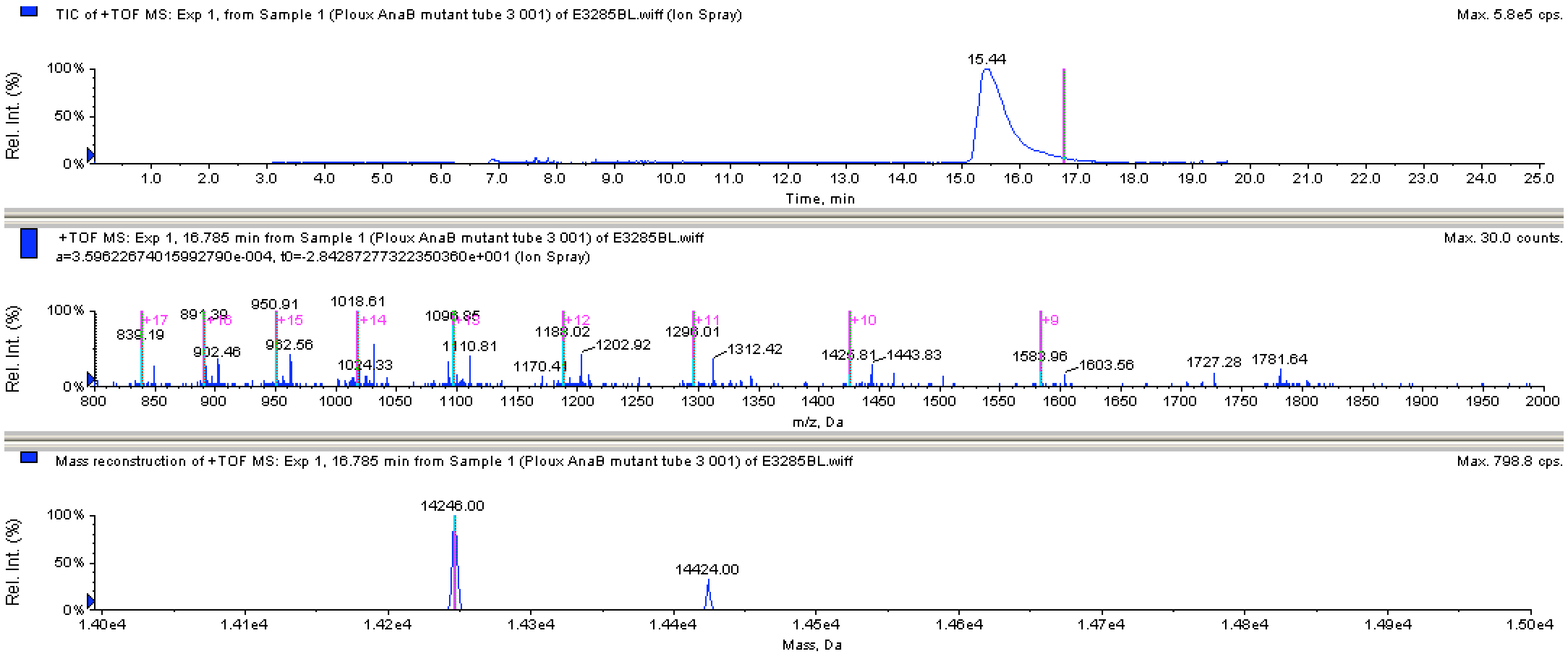

	Mass (avg.)	Mass (mono.)	Apex Mass	Area	Start Scan	Stop Scan	Score	Evidence
1	14246.7163		14246.9365	4667.0000	920	920	1.0000	C

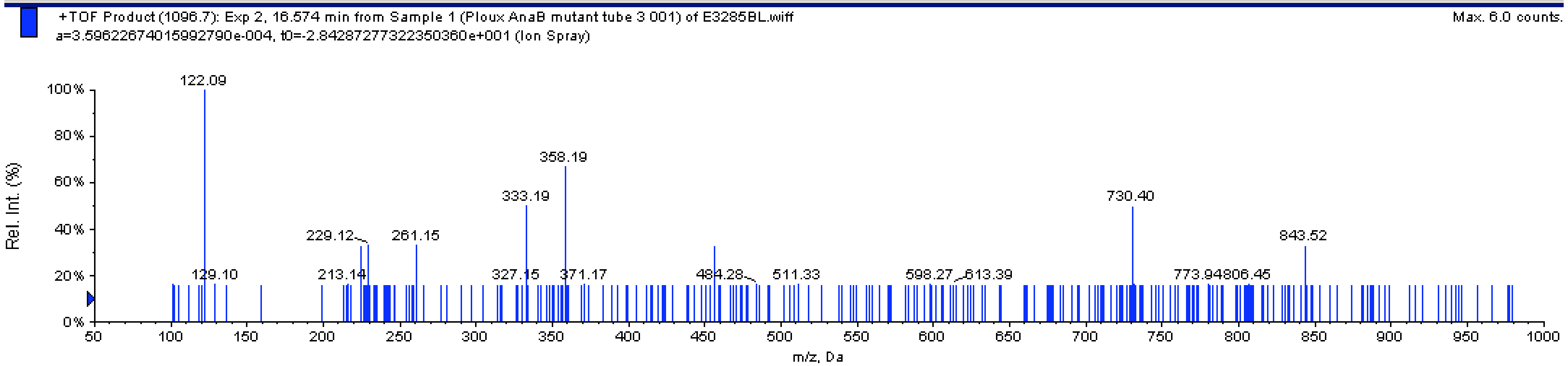

Figure S5C.

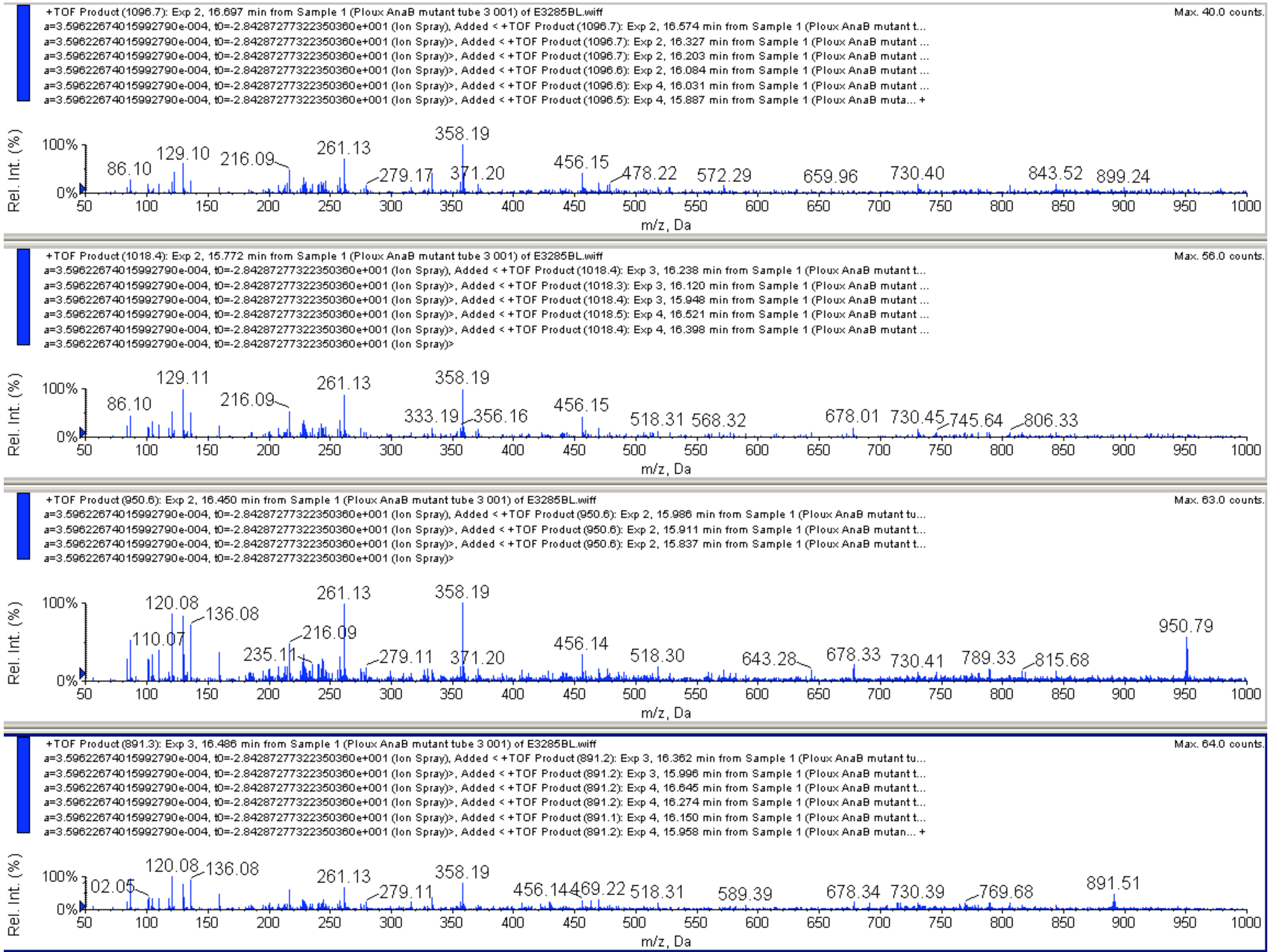
+TOF Product (1096.7): Exp 2, 16.697 min from Sample 1 (Ploux AnaB mutant tube 3 001) of E3285BL.wiff
Max. 40.0 counts.
Rel. Int. (%)
100%
0%
86.10
129.10
216.09
261.13
279.17
358.19
371.20
456.15
478.22
572.29
659.96
730.40
843.52
899.24
m/z, Da
+TOF Product (1018.4): Exp 2, 15.772 min from Sample 1 (Ploux AnaB mutant tube 3 001) of E3285BL.wiff
Max. 56.0 counts.
86.10
129.11
216.09
261.13
333.19
356.16
358.19
456.15
518.31
568.32
678.01
730.45
745.64
806.33
+TOF Product (950.6): Exp 2, 16.450 min from Sample 1 (Ploux AnaB mutant tube 3 001) of E3285BL.wiff
Max. 63.0 counts.
110.07
120.08
136.08
216.09
235.11
261.13
279.11
358.19
371.20
456.14
518.30
643.28
678.33
730.41
789.33
815.68
950.79
+TOF Product (891.3): Exp 3, 16.486 min from Sample 1 (Ploux AnaB mutant tube 3 001) of E3285BL.wiff
Max. 64.0 counts.
102.05
120.08
136.08
261.13
279.11
358.19
456.14
469.22
518.31
589.39
678.34
730.39
769.68
891.51
50 100 150 200 250 300 350 400 450 500 550 600 650 700 750 800 850 900 950 1000

Figure S6A.

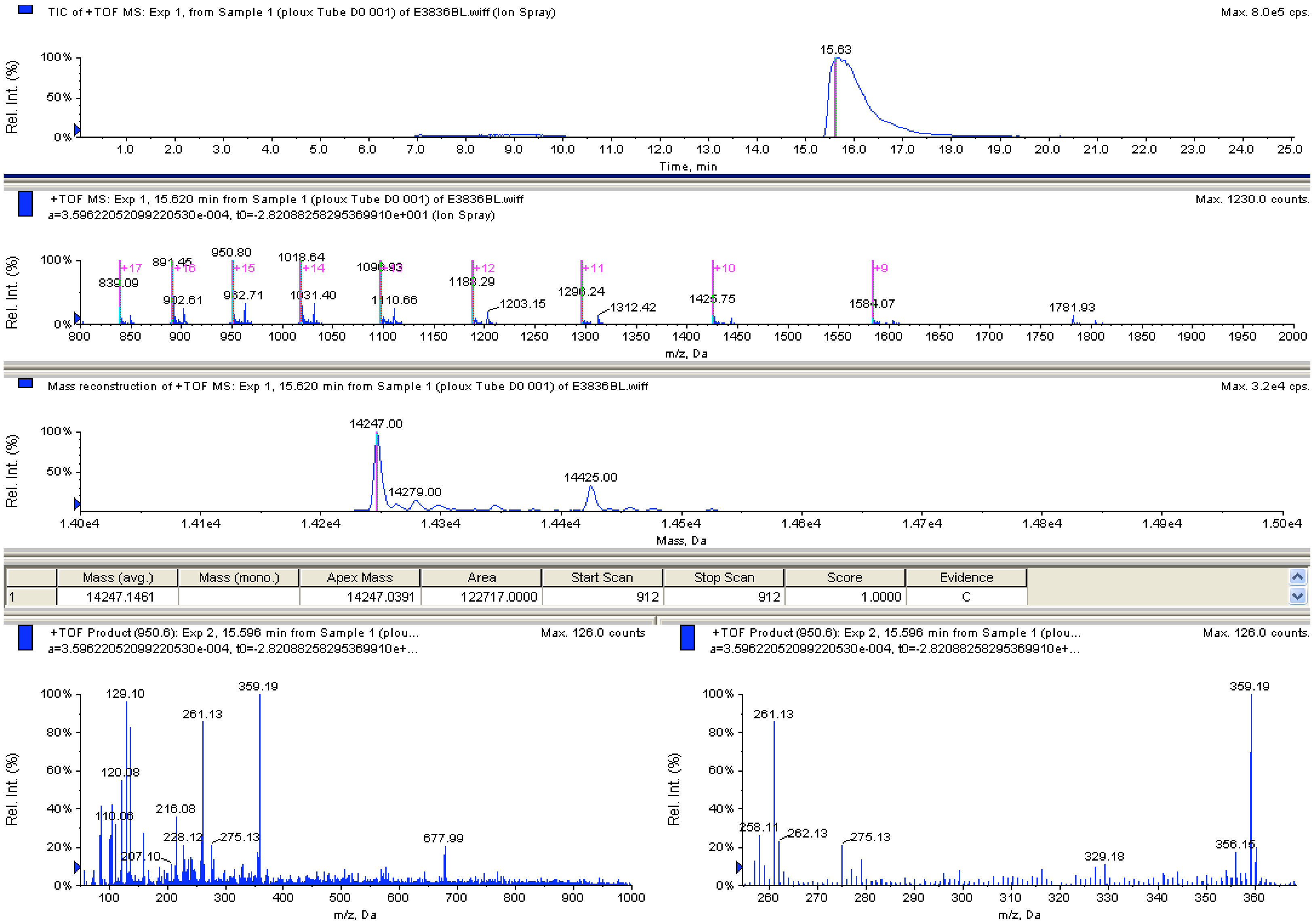
TIC of +TOF MS: Exp 1, from Sample 1 (ploux Tube D0 001) of E3836BL.wiff (Ion Spray)
Max. 8.0e5 cps.
15.63
Rel. Int. (%)
Time, min
+TOF MS: Exp 1, 15.620 min from Sample 1 (ploux Tube D0 001) of E3836BL.wiff
a=3.59622052099220530e-004, t0=-2.82088258295369910e+001 (Ion Spray)
Max. 1230.0 counts.
839.09
891.45
950.80
1018.64
1096.93
1188.29
1296.24
1425.75
1584.07
1781.93
902.61
962.71
1031.40
1110.66
1203.15
1312.42
+17
+16
+15
+14
+12
+11
+10
+9
m/z, Da
Mass reconstruction of +TOF MS: Exp 1, 15.620 min from Sample 1 (ploux Tube D0 001) of E3836BL.wiff
Max. 3.2e4 cps.
14247.00
14279.00
14425.00
Mass, Da
Mass (avg.)
Mass (mono.)
Apex Mass
Area
Start Scan
Stop Scan
Score
Evidence
1
14247.1461
14247.0391
122717.0000
912
912
1.0000
C
+TOF Product (950.6): Exp 2, 15.596 min from Sample 1 (plou...
a=3.59622052099220530e-004, t0=-2.82088258295369910e+...
Max. 126.0 counts.
129.10
359.19
261.13
120.08
110.06
216.08
228.12
275.13
207.10
677.99
258.11
262.13
329.18
356.15

Figure S6B.

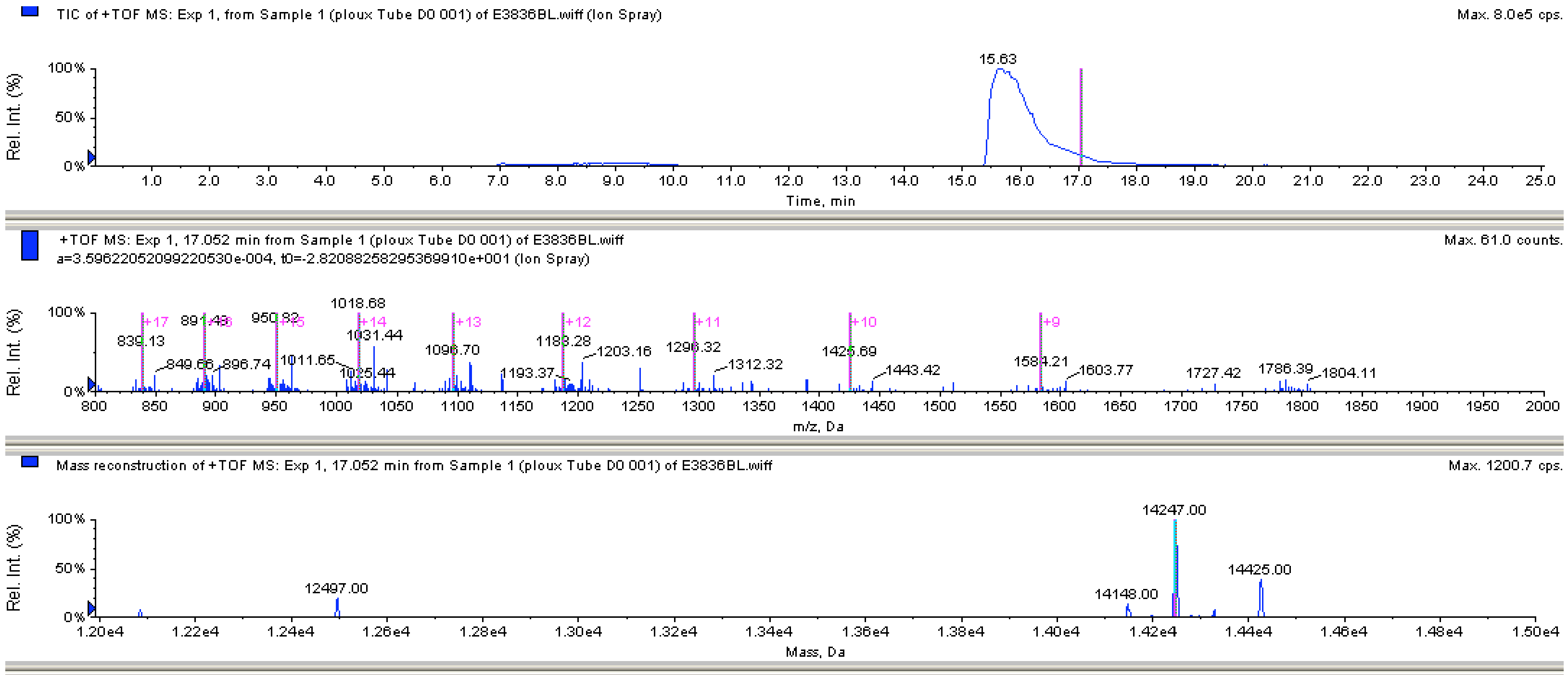

	Mass (avg.)	Mass (mono.)	Apex Mass	Area	Start Scan	Stop Scan	Score	Evidence
1	14247.4378		14247.5031	8753.0000	940	940	1.0000	C

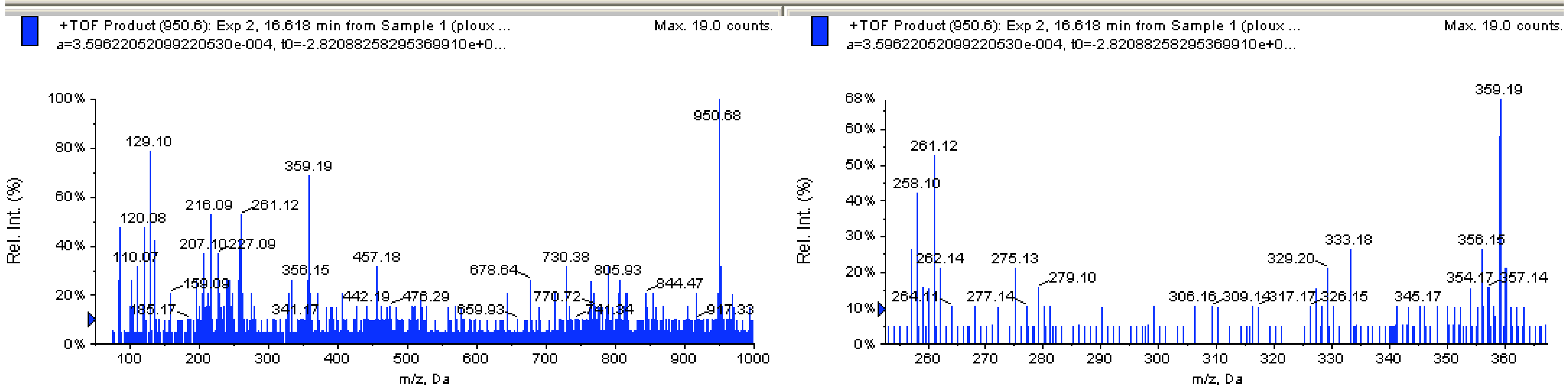

Figure S7A.

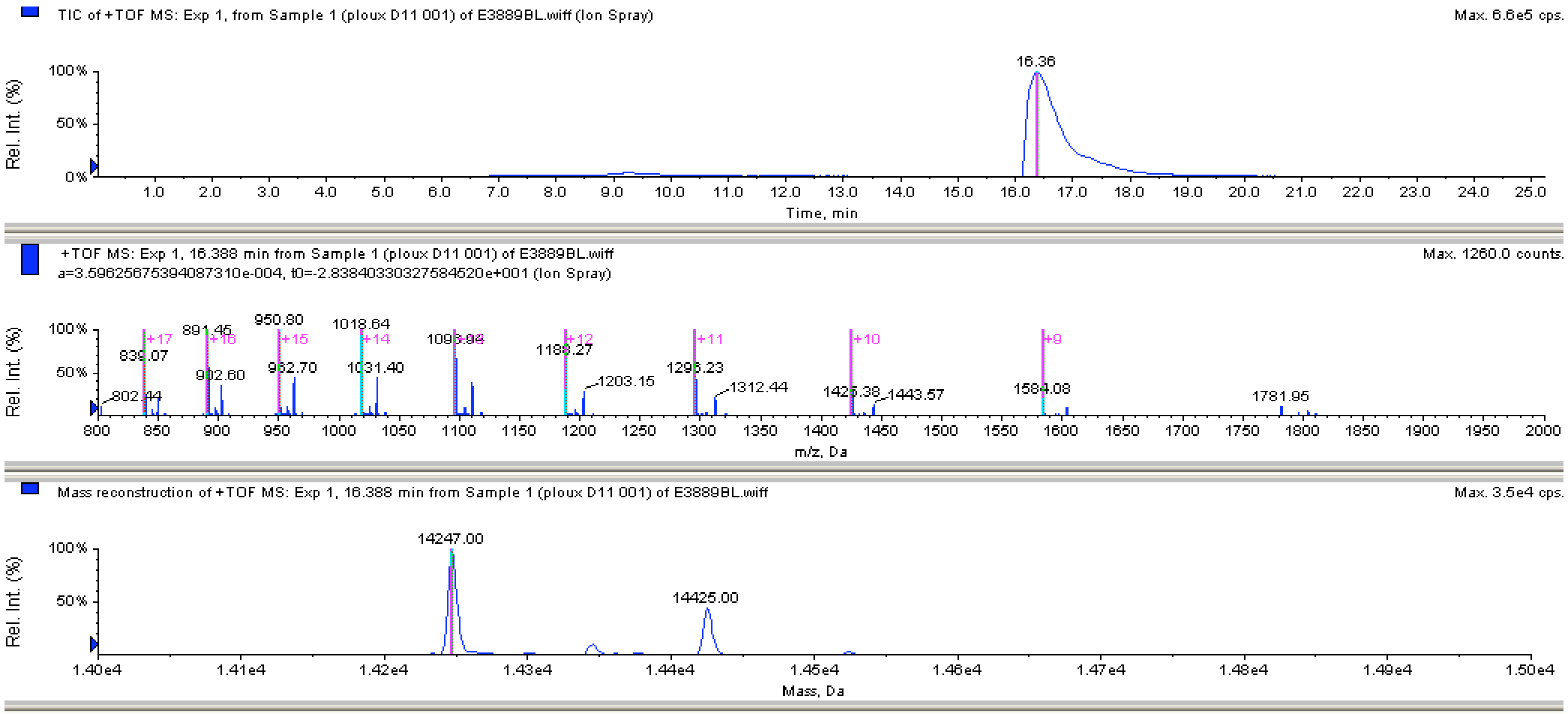

	Mass (avg.)	Mass (mono.)	Apex Mass	Area	Start Scan	Stop Scan	Score	Evidence
1	14247.2071		14247.1695	129697.0000	955	955	1.0000	C

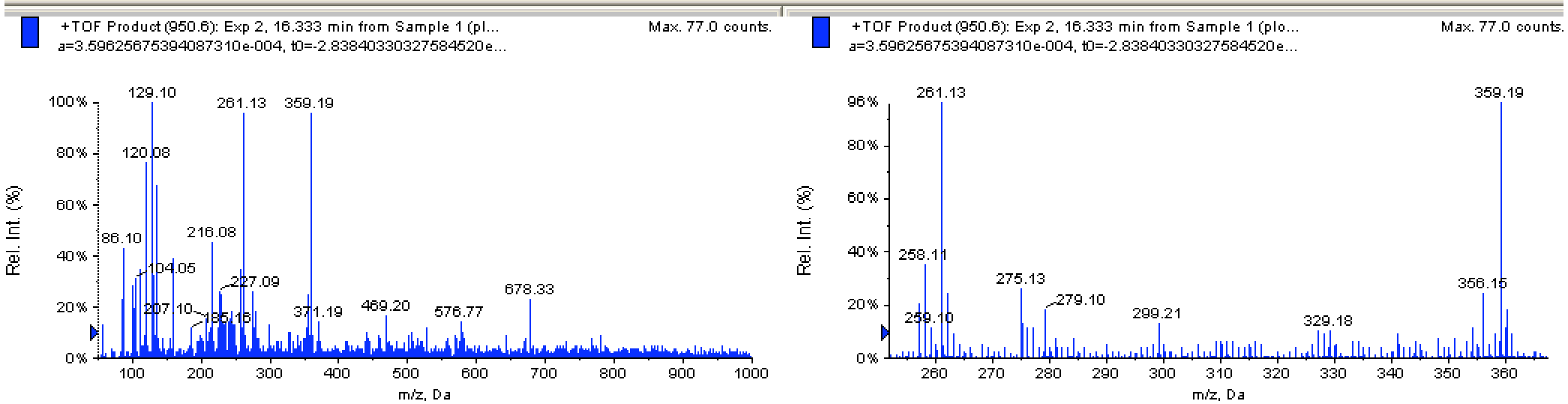

Figure S7B.

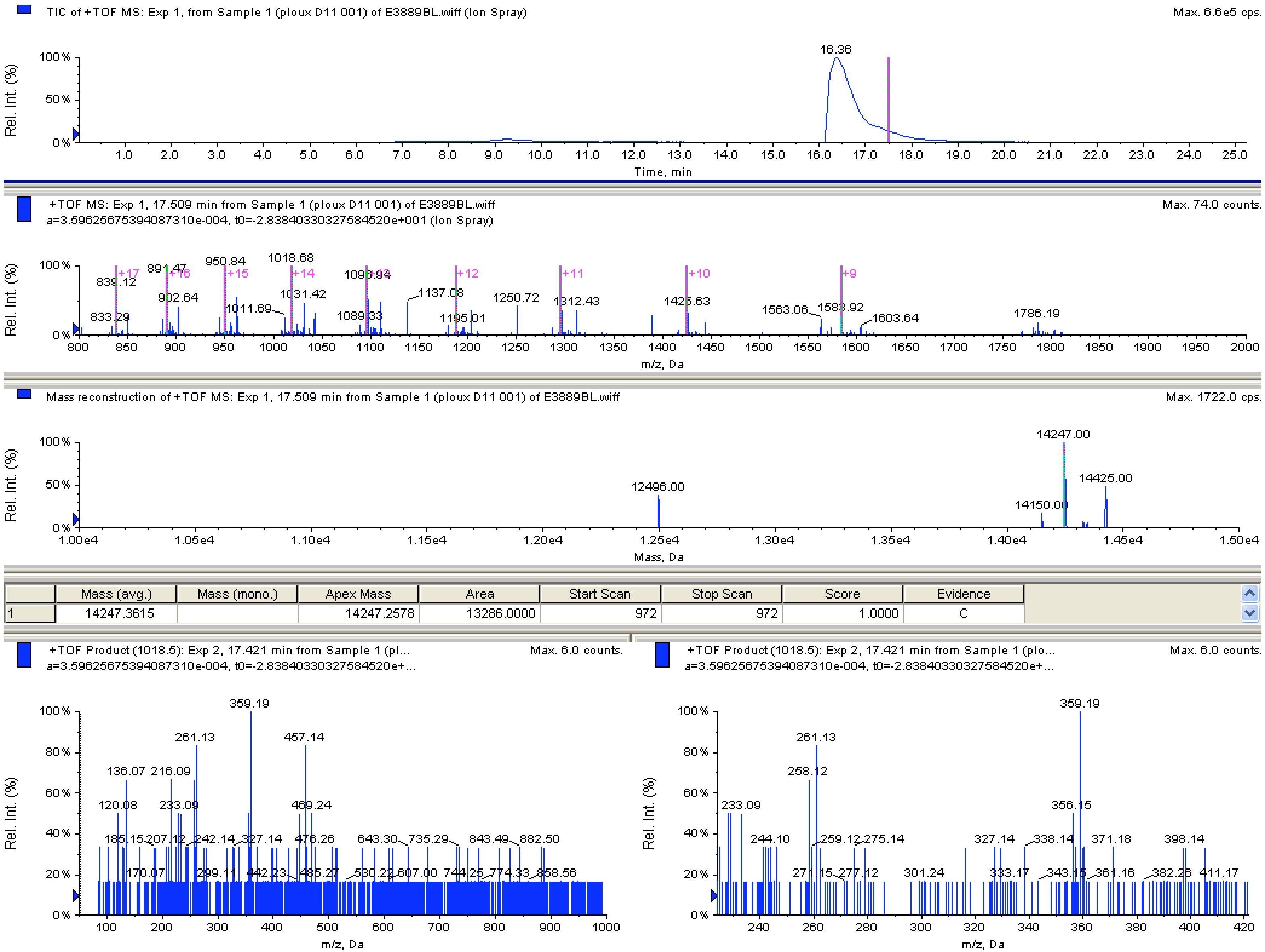
TIC of +TOF MS: Exp 1, from Sample 1 (ploux D11 001) of E3889BL.wiff (Ion Spray)
Max. 6.6e5 cps.
16.36
Rel. Int. (%)
Time, min
+TOF MS: Exp 1, 17.509 min from Sample 1 (ploux D11 001) of E3889BL.wiff
a=3.59625675394087310e-004, t0=-2.83840330327584520e+001 (Ion Spray)
Max. 74.0 counts.
+17 +16 +15 +14 +13 +12 +11 +10 +9
833.29
839.12
891.47
902.64
950.84
1011.69
1018.68
1031.42
1089.33
1137.08
1195.01
1250.72
1312.43
1563.06
1603.64
1786.19
m/z, Da
Mass reconstruction of +TOF MS: Exp 1, 17.509 min from Sample 1 (ploux D11 001) of E3889BL.wiff
Max. 1722.0 cps.
14247.00
14425.00
12496.00
14150.00
Mass, Da
Mass (avg.) | Mass (mono.) | Apex Mass | Area | Start Scan | Stop Scan | Score | Evidence
1 | 14247.3615 | | 14247.2578 | 13286.0000 | 972 | 972 | 1.0000 | C
+TOF Product (1018.5): Exp 2, 17.421 min from Sample 1 (pl...
a=3.59625675394087310e-004, t0=-2.83840330327584520e+...
Max. 6.0 counts.
359.19
261.13
457.14
136.07
216.09
120.08
233.09
469.24
185.15
207.12
242.14
327.14
476.26
643.30
735.29
843.49
882.50
170.07
299.11
442.23
485.27
530.22
607.00
744.25
774.33
858.56
m/z, Da
+TOF Product (1018.5): Exp 2, 17.421 min from Sample 1 (plo...
a=3.59625675394087310e-004, t0=-2.83840330327584520e+...
Max. 6.0 counts.
359.19
261.13
258.12
233.09
356.15
244.10
259.12
275.14
327.14
338.14
371.18
398.14
271.15
277.12
301.24
333.17
343.15
361.16
382.26
411.17
m/z, Da

Figure S8A.

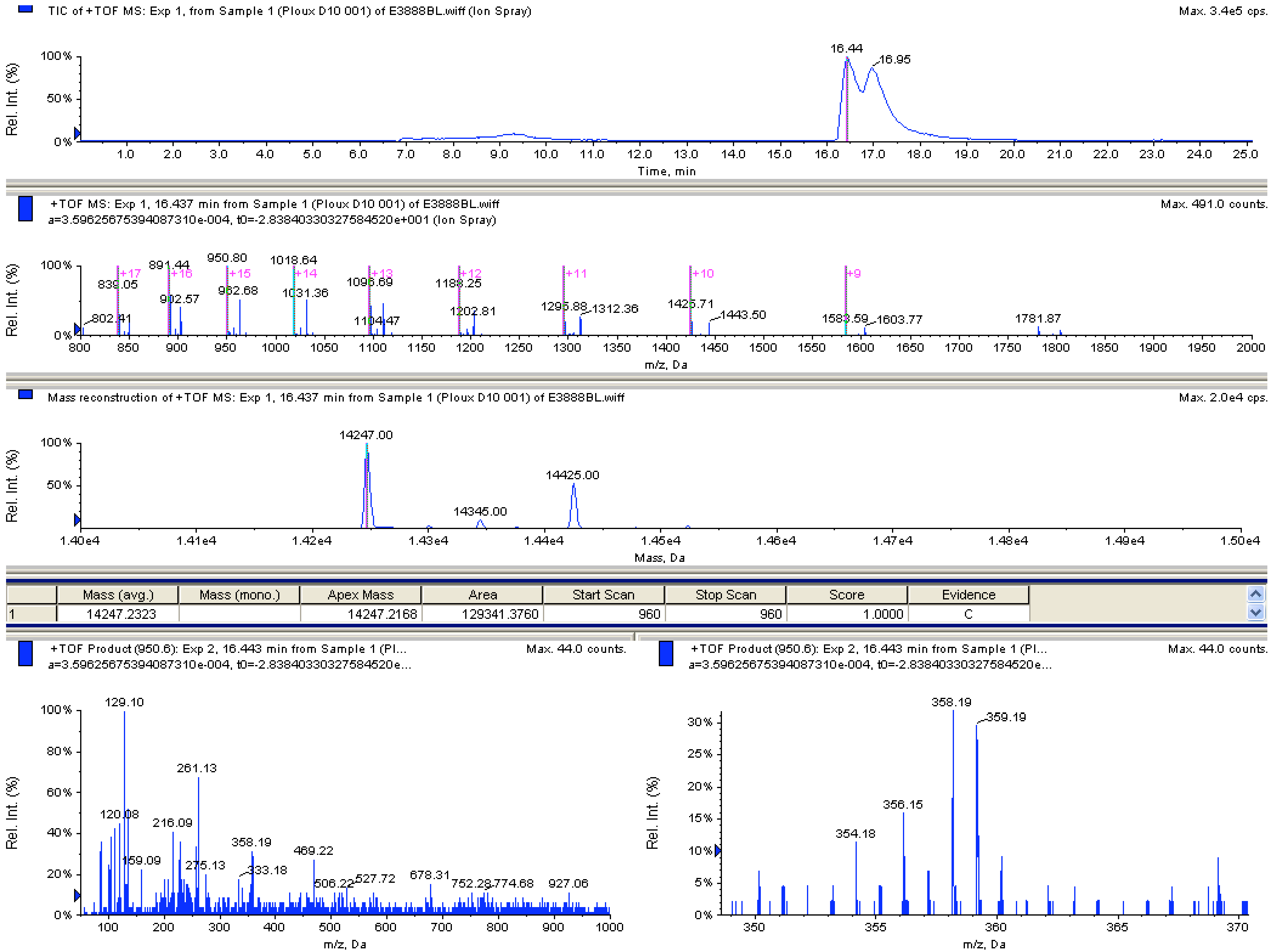
TIC of +TOF MS: Exp 1, from Sample 1 (Ploux D10 001) of E3888BL.wiff (Ion Spray)
Max. 3.4e5 cps.
16.44
16.95
Time, min
Rel. Int. (%)
+TOF MS: Exp 1, 16.437 min from Sample 1 (Ploux D10 001) of E3888BL.wiff
a=3.59625675394087310e-004, t0=-2.83840330327584520e+001 (Ion Spray)
Max. 491.0 counts.
+17 +16 +15 +14 +13 +12 +11 +10 +9
891.44 950.80 1018.64 839.05 902.57 962.68 1031.36 1096.69 1188.25 1202.81 1104.47 802.41 1295.88 1312.36 1425.71 1443.50 1583.59 1603.77 1781.87
m/z, Da
Mass reconstruction of +TOF MS: Exp 1, 16.437 min from Sample 1 (Ploux D10 001) of E3888BL.wiff
Max. 2.0e4 cps.
14247.00
14425.00
14345.00
Mass, Da
Mass (avg.) | Mass (mono.) | Apex Mass | Area | Start Scan | Stop Scan | Score | Evidence
1 | 14247.2323 | | 14247.2168 | 129341.3760 | 960 | 960 | 1.0000 | C
+TOF Product (950.6): Exp 2, 16.443 min from Sample 1 (Pl...
a=3.59625675394087310e-004, t0=-2.83840330327584520e...
Max. 44.0 counts.
129.10 261.13 120.08 216.09 159.09 275.13 358.19 333.18 469.22 506.22 527.72 678.31 752.28 774.68 927.06
358.19 359.19 356.15 354.18
m/z, Da

Figure S8B.

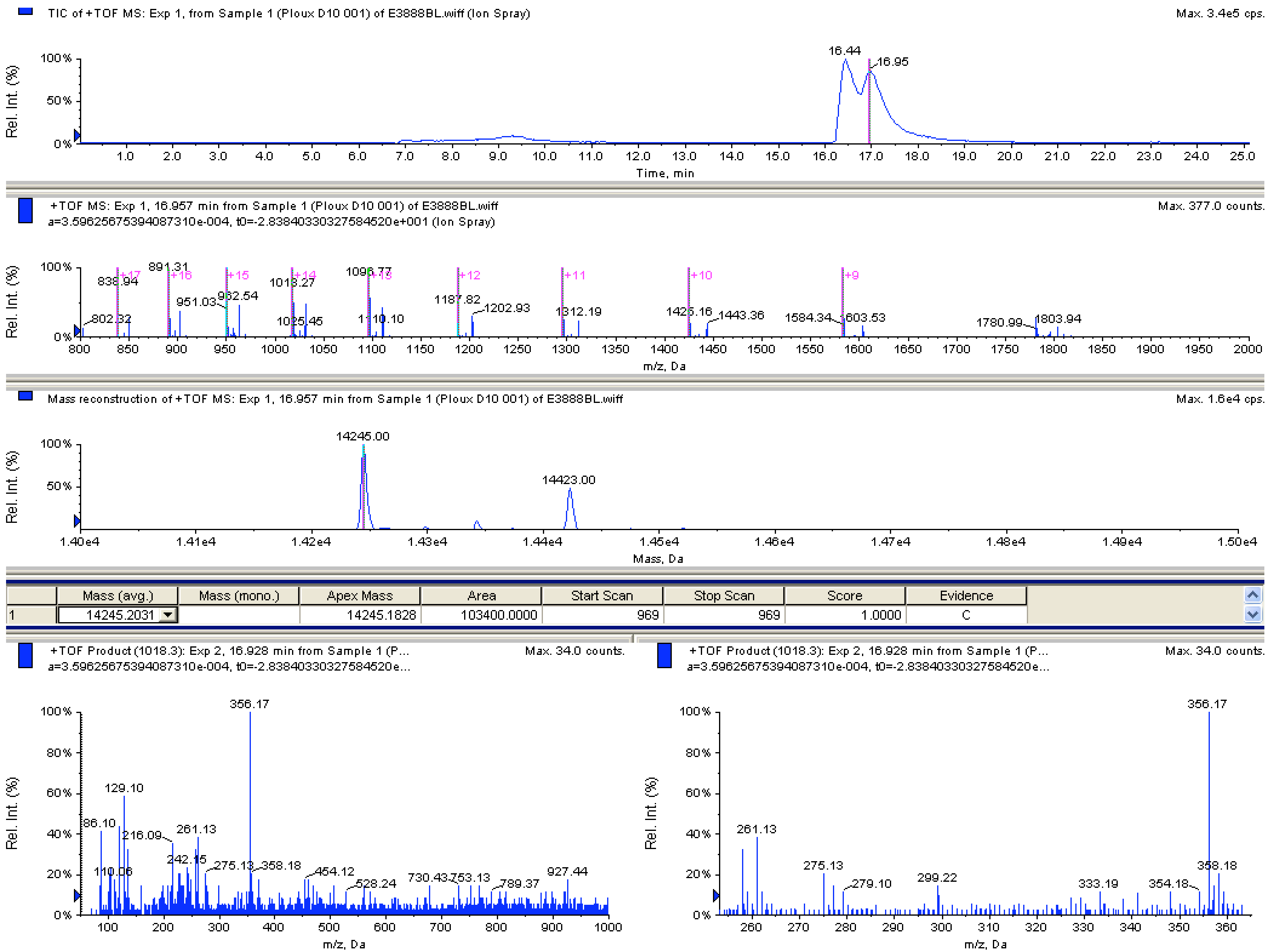
TIC of +TOF MS: Exp 1, from Sample 1 (Ploux D10 001) of E3888BL.wiff (Ion Spray)
Max. 3.4e5 cps.
16.44
16.95
Time, min
+TOF MS: Exp 1, 16.957 min from Sample 1 (Ploux D10 001) of E3888BL.wiff
a=3.59625675394087310e-004, t0=-2.83840330327584520e+001 (Ion Spray)
Max. 377.0 counts.
m/z, Da
Mass reconstruction of +TOF MS: Exp 1, 16.957 min from Sample 1 (Ploux D10 001) of E3888BL.wiff
Max. 1.6e4 cps.
14245.00
14423.00
Mass, Da
Mass (avg.)
Mass (mono.)
Apex Mass
Area
Start Scan
Stop Scan
Score
Evidence
1
14245.2031
14245.1828
103400.0000
969
969
1.0000
C
+TOF Product (1018.3): Exp 2, 16.928 min from Sample 1 (P...
a=3.59625675394087310e-004, t0=-2.83840330327584520e...
Max. 34.0 counts.
356.17
129.10
261.13
m/z, Da
Rel. Int. (%)

Figure S9A.

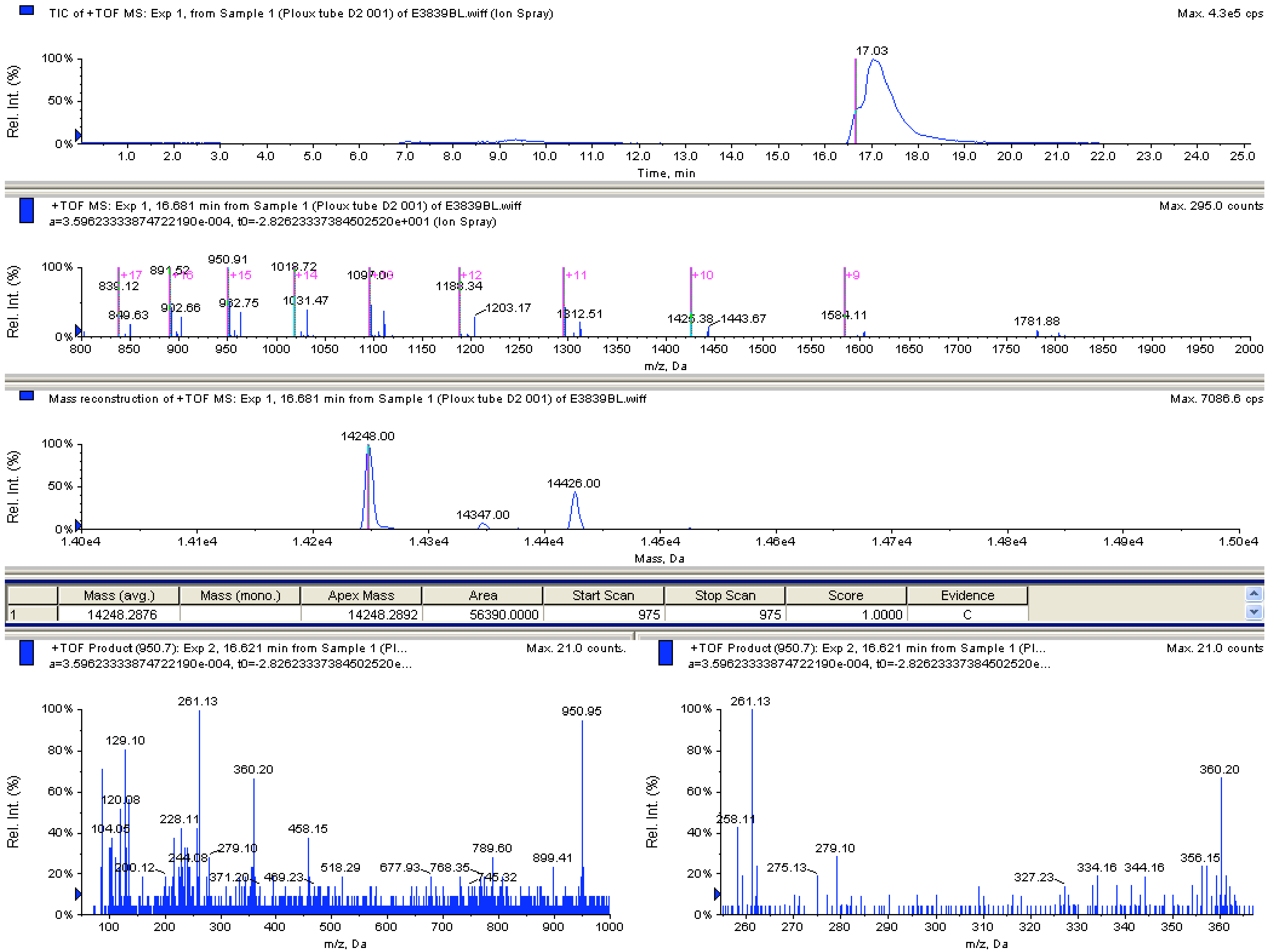
TIC of +TOF MS: Exp 1, from Sample 1 (Ploux tube D2 001) of E3839BL.wiff (Ion Spray)
Max. 4.3e5 cps
17.03
Rel. Int. (%)
Time, min
+TOF MS: Exp 1, 16.681 min from Sample 1 (Ploux tube D2 001) of E3839BL.wiff
a=3.59623333874722190e-004, t0=-2.82623337384502520e+001 (Ion Spray)
Max. 295.0 counts
950.91
1018.72
1188.34
1203.17
1312.51
1443.67
1584.11
1781.88
m/z, Da
Mass reconstruction of +TOF MS: Exp 1, 16.681 min from Sample 1 (Ploux tube D2 001) of E3839BL.wiff
Max. 7086.6 cps
14248.00
14347.00
14426.00
Mass, Da
Mass (avg.) | Mass (mono.) | Apex Mass | Area | Start Scan | Stop Scan | Score | Evidence
1 | 14248.2876 | | 14248.2892 | 56390.0000 | 975 | 975 | 1.0000 | C
+TOF Product (950.7): Exp 2, 16.621 min from Sample 1 (Pl...
a=3.59623333874722190e-004, t0=-2.82623337384502520e...
Max. 21.0 counts
261.13
129.10
360.20
120.08
228.11
104.06
458.15
279.10
789.60
899.41
950.95
518.29
677.93
768.35
745.32
371.20
469.23
244.08
200.12
m/z, Da
258.11
275.13
327.23
334.16
344.16
356.15

Figure S9B.

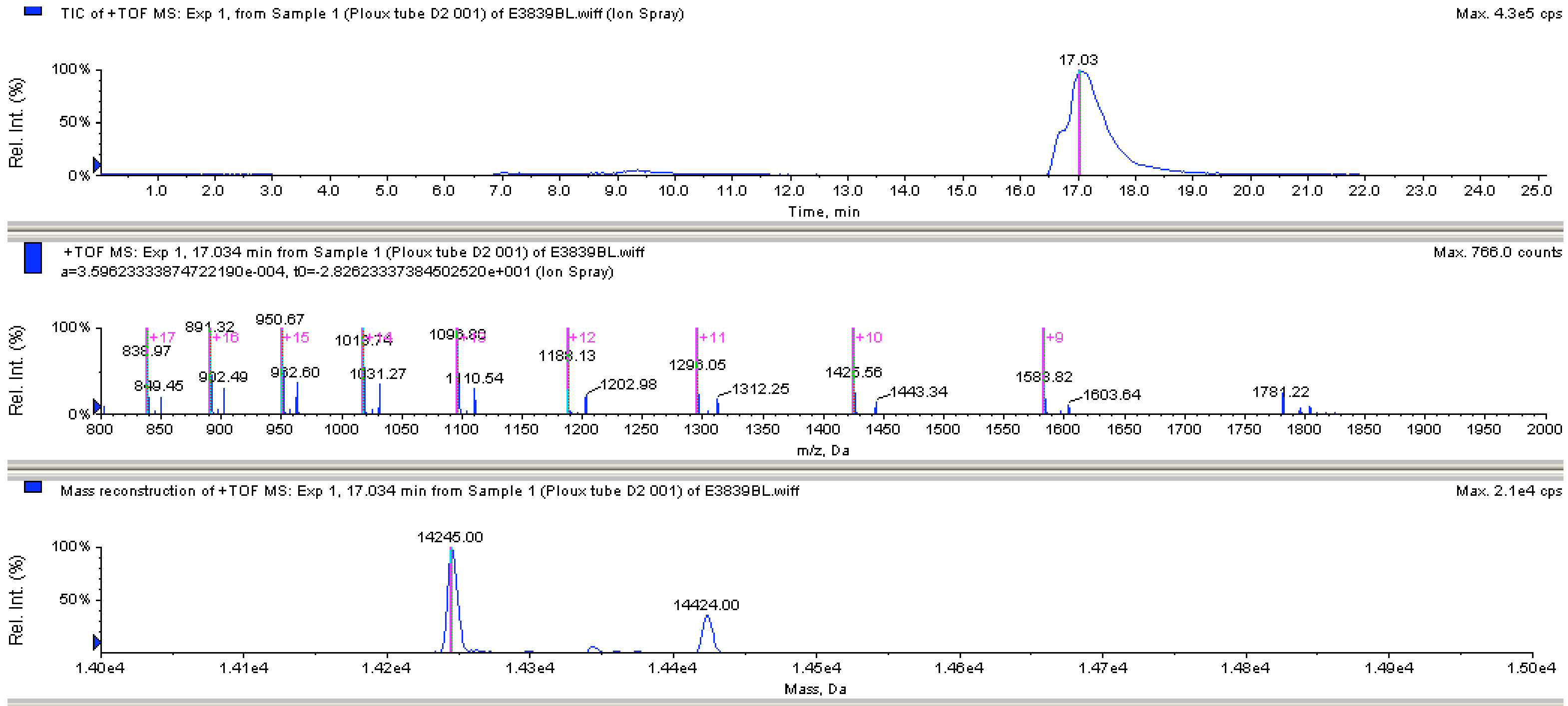

	Mass (avg.)	Mass (mono.)	Apex Mass	Area	Start Scan	Stop Scan	Score	Evidence
1	14245.4257		14245.4098	161128.0000	982	982	1.0000	C

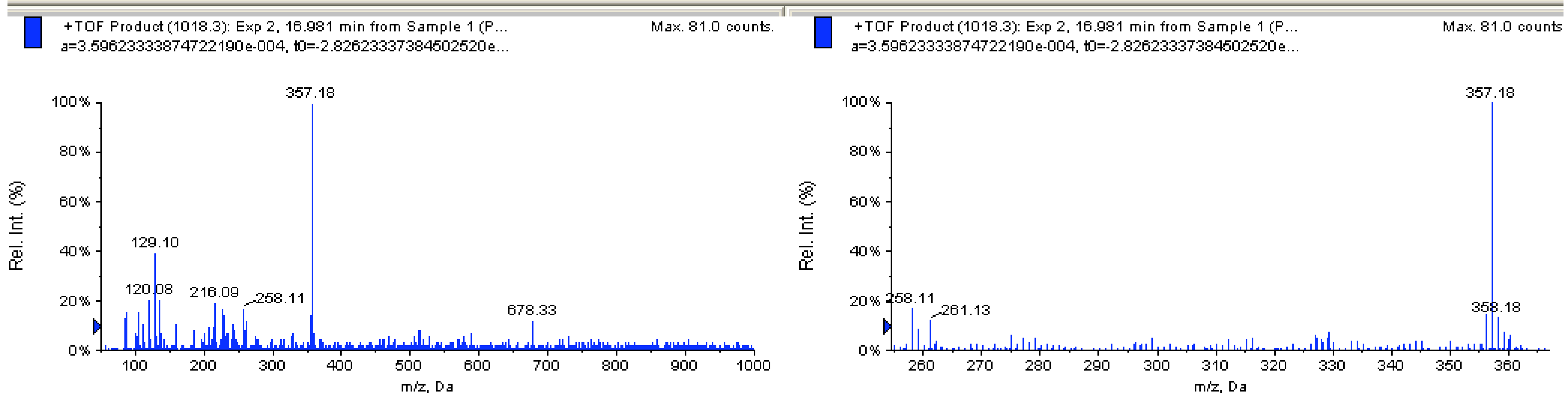

Figure S10A.

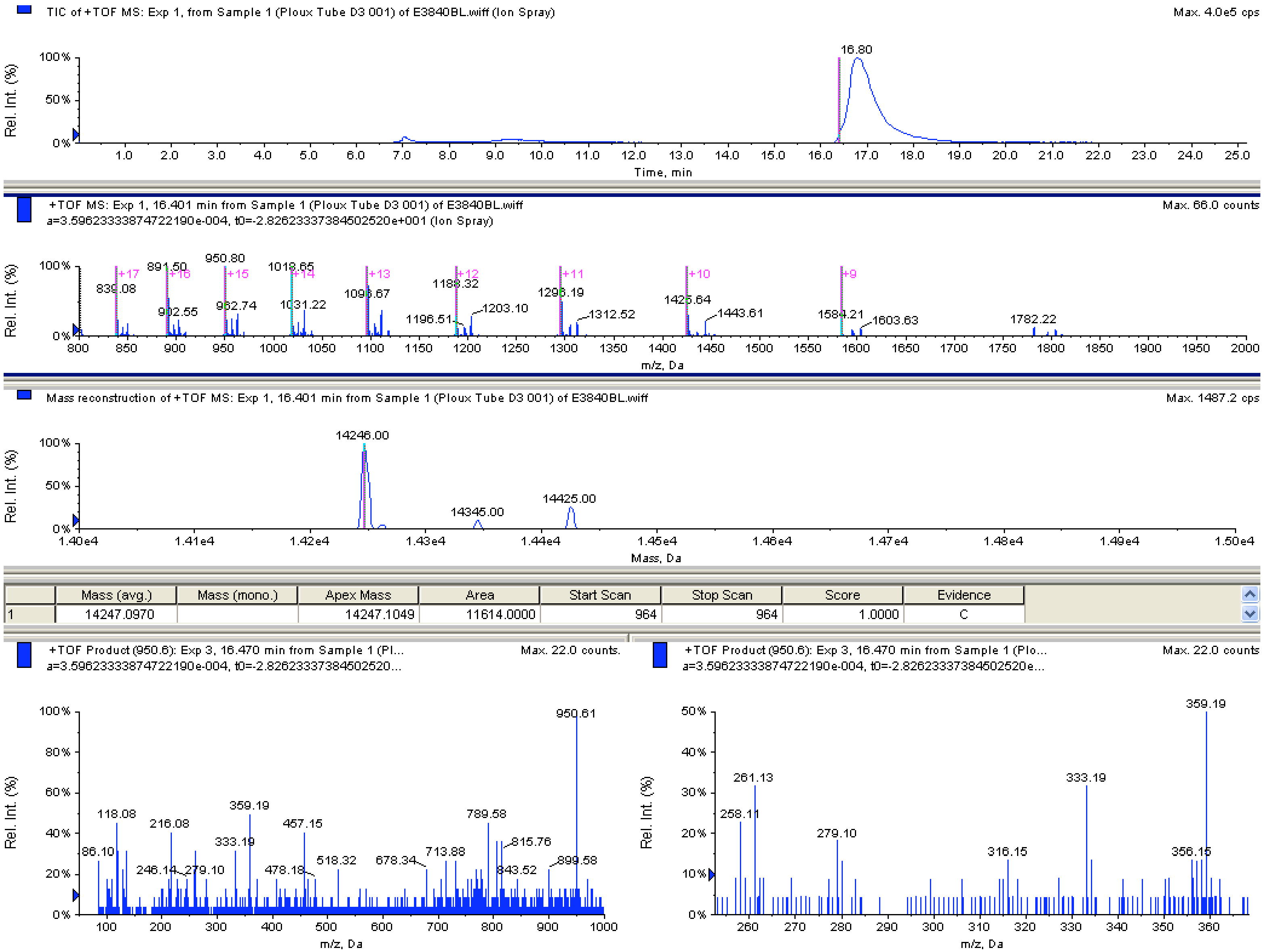
TIC of +TOF MS: Exp 1, from Sample 1 (Ploux Tube D3 001) of E3840BL.wiff (Ion Spray)
Max. 4.0e5 cps
16.80
Rel. Int. (%)
Time, min
+TOF MS: Exp 1, 16.401 min from Sample 1 (Ploux Tube D3 001) of E3840BL.wiff
a=3.59623333874722190e-004, t0=-2.82623337384502520e+001 (Ion Spray)
Max. 66.0 counts
839.08
891.50
950.80
1018.65
1098.67
1188.32
1296.19
1425.64
1584.21
902.55
962.74
1031.22
1196.51
1203.10
1312.52
1443.61
1603.63
1782.22
+17
+16
+15
+14
+13
+12
+11
+10
+9
m/z, Da
Mass reconstruction of +TOF MS: Exp 1, 16.401 min from Sample 1 (Ploux Tube D3 001) of E3840BL.wiff
Max. 1487.2 cps
14246.00
14345.00
14425.00
Mass, Da
| | Mass (avg.) | Mass (mono.) | Apex Mass | Area | Start Scan | Stop Scan | Score | Evidence |
| 1 | 14247.0970 | | 14247.1049 | 11614.0000 | 964 | 964 | 1.0000 | C |
+TOF Product (950.6): Exp 3, 16.470 min from Sample 1 (Pl...
a=3.59623333874722190e-004, t0=-2.82623337384502520...
Max. 22.0 counts.
950.61
118.08
216.08
359.19
457.15
789.58
333.19
815.76
86.10
246.14
279.10
478.18
518.32
678.34
713.88
843.52
899.58
m/z, Da
+TOF Product (950.6): Exp 3, 16.470 min from Sample 1 (Plo...
a=3.59623333874722190e-004, t0=-2.82623337384502520e...
Max. 22.0 counts
359.19
261.13
333.19
258.11
279.10
316.15
356.15
m/z, Da

Figure S10B.

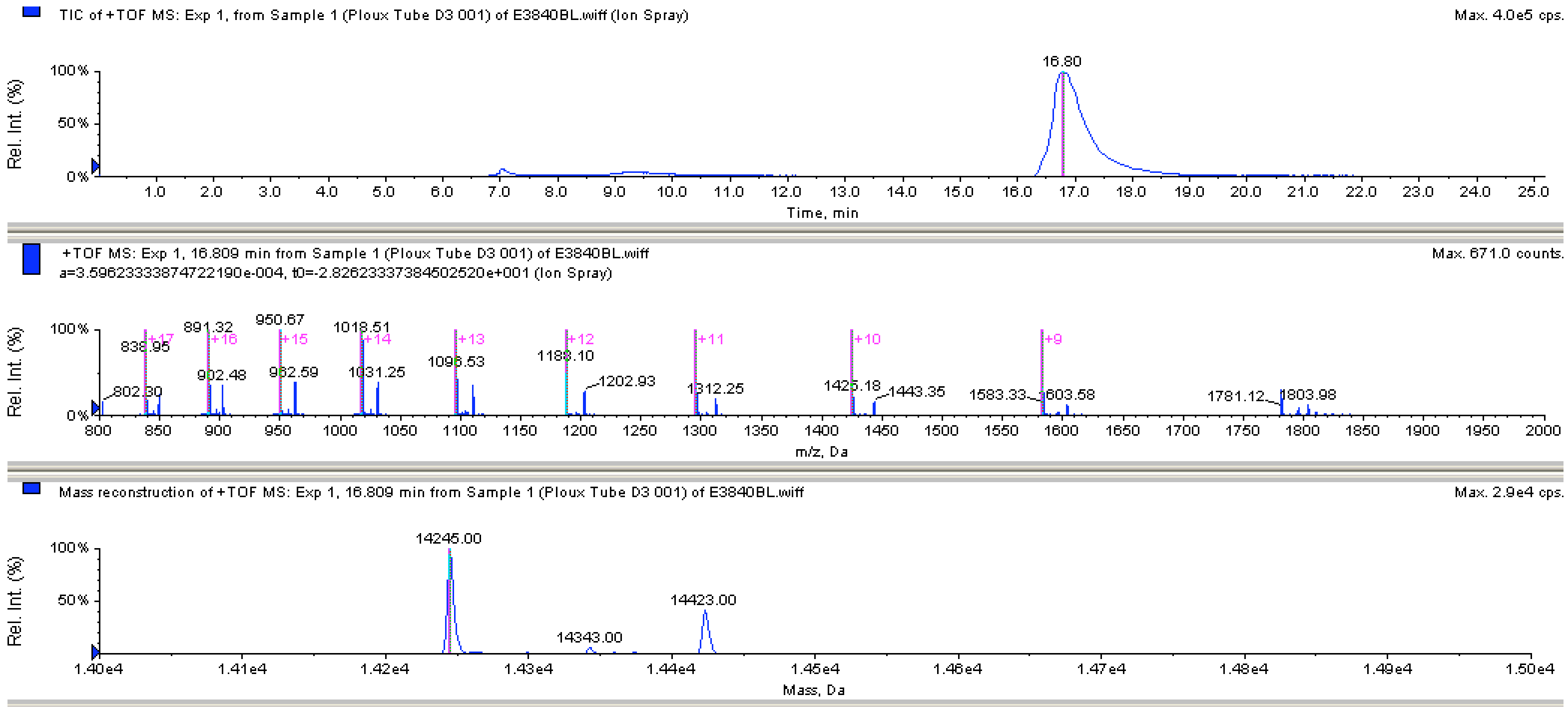

	Mass (avg.)	Mass (mono.)	Apex Mass	Area	Start Scan	Stop Scan	Score	Evidence
1	14245.5764		14245.5243	179272.8916	972	972	1.0000	C

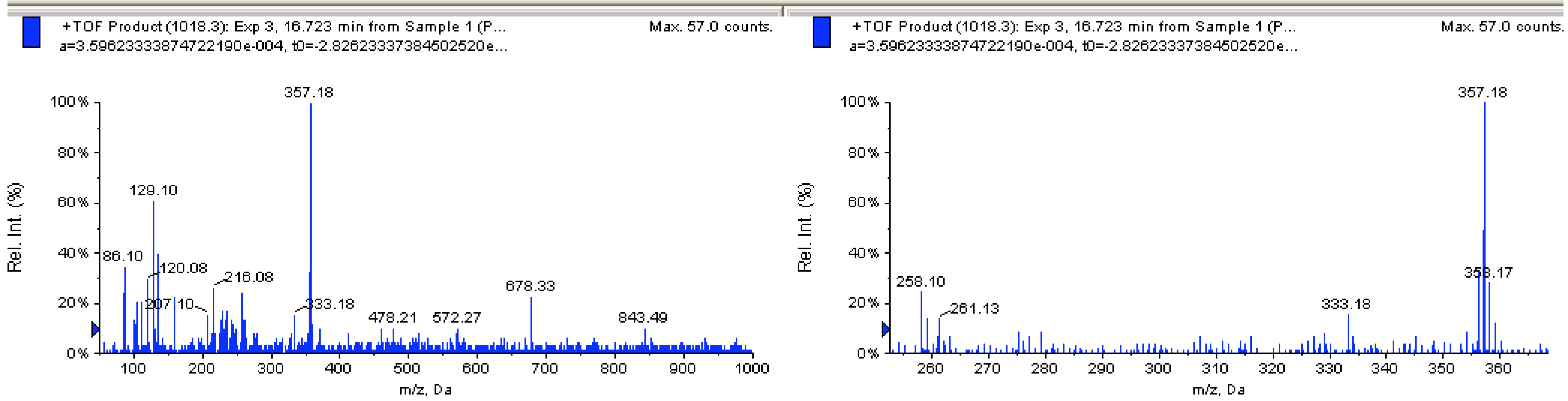

Figure S11A.

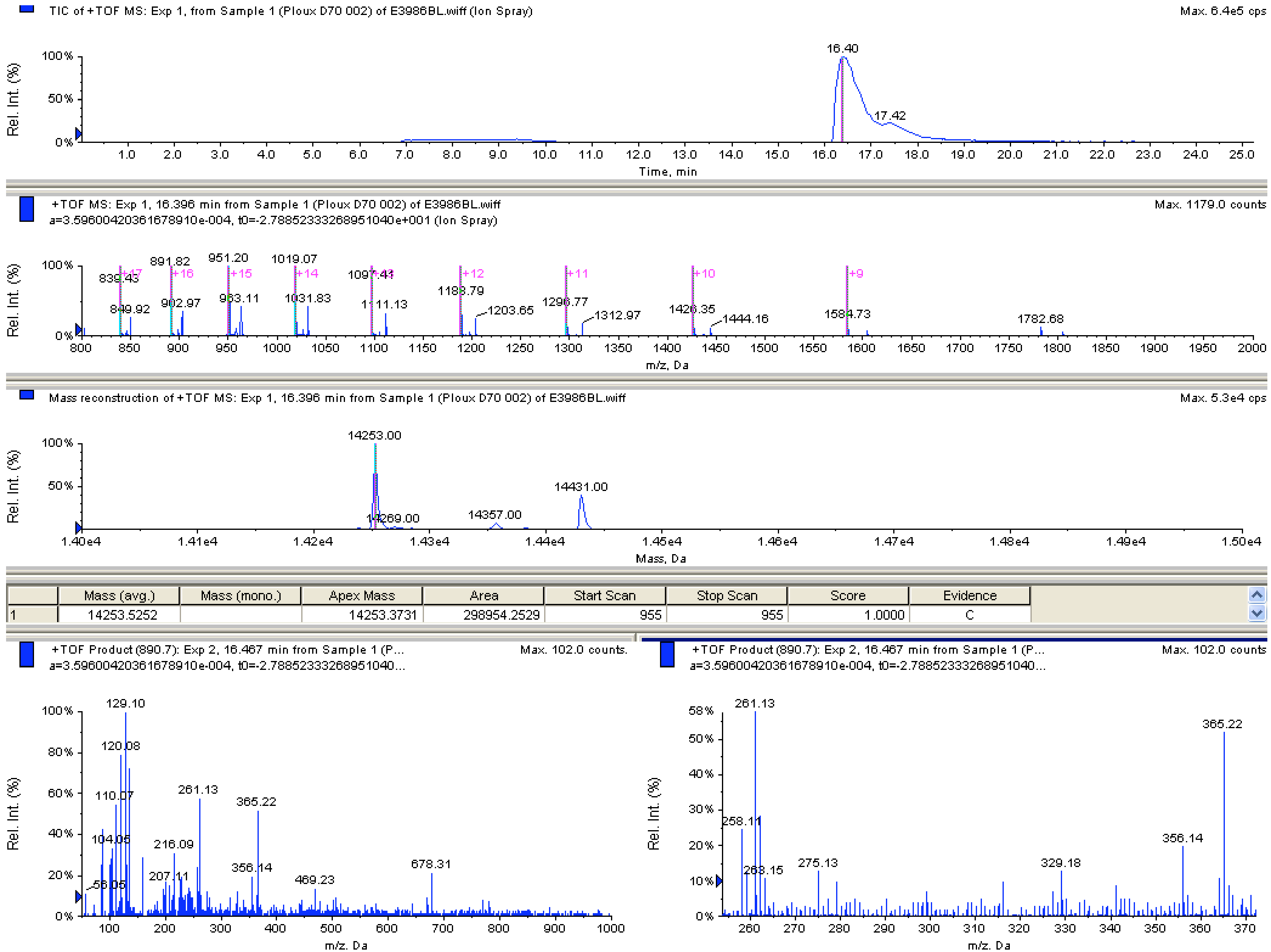
TIC of +TOF MS: Exp 1, from Sample 1 (Ploux D70 002) of E3986BL.wiff (Ion Spray)
Max. 6.4e5 cps
16.40
17.42
Rel. Int. (%)
Time, min
+TOF MS: Exp 1, 16.396 min from Sample 1 (Ploux D70 002) of E3986BL.wiff
a=3.59600420361678910e-004, t0=-2.78852333268951040e+001 (Ion Spray)
Max. 1179.0 counts
891.82
951.20
1019.07
839.43
849.92
902.97
963.11
1031.83
1188.79
1203.65
1296.77
1312.97
1426.35
1444.16
1584.73
1782.68
m/z, Da
Mass reconstruction of +TOF MS: Exp 1, 16.396 min from Sample 1 (Ploux D70 002) of E3986BL.wiff
Max. 5.3e4 cps
14253.00
14269.00
14357.00
14431.00
Mass, Da
Mass (avg.) | Mass (mono.) | Apex Mass | Area | Start Scan | Stop Scan | Score | Evidence
1 | 14253.5252 | | 14253.3731 | 298954.2529 | 955 | 955 | 1.0000 | C
+TOF Product (890.7): Exp 2, 16.467 min from Sample 1 (P...
a=3.59600420361678910e-004, t0=-2.78852333268951040...
Max. 102.0 counts.
129.10
120.08
110.07
104.05
56.05
261.13
216.09
207.11
365.22
356.14
469.23
678.31
258.11
263.15
275.13
329.18
m/z, Da

Figure S11B.

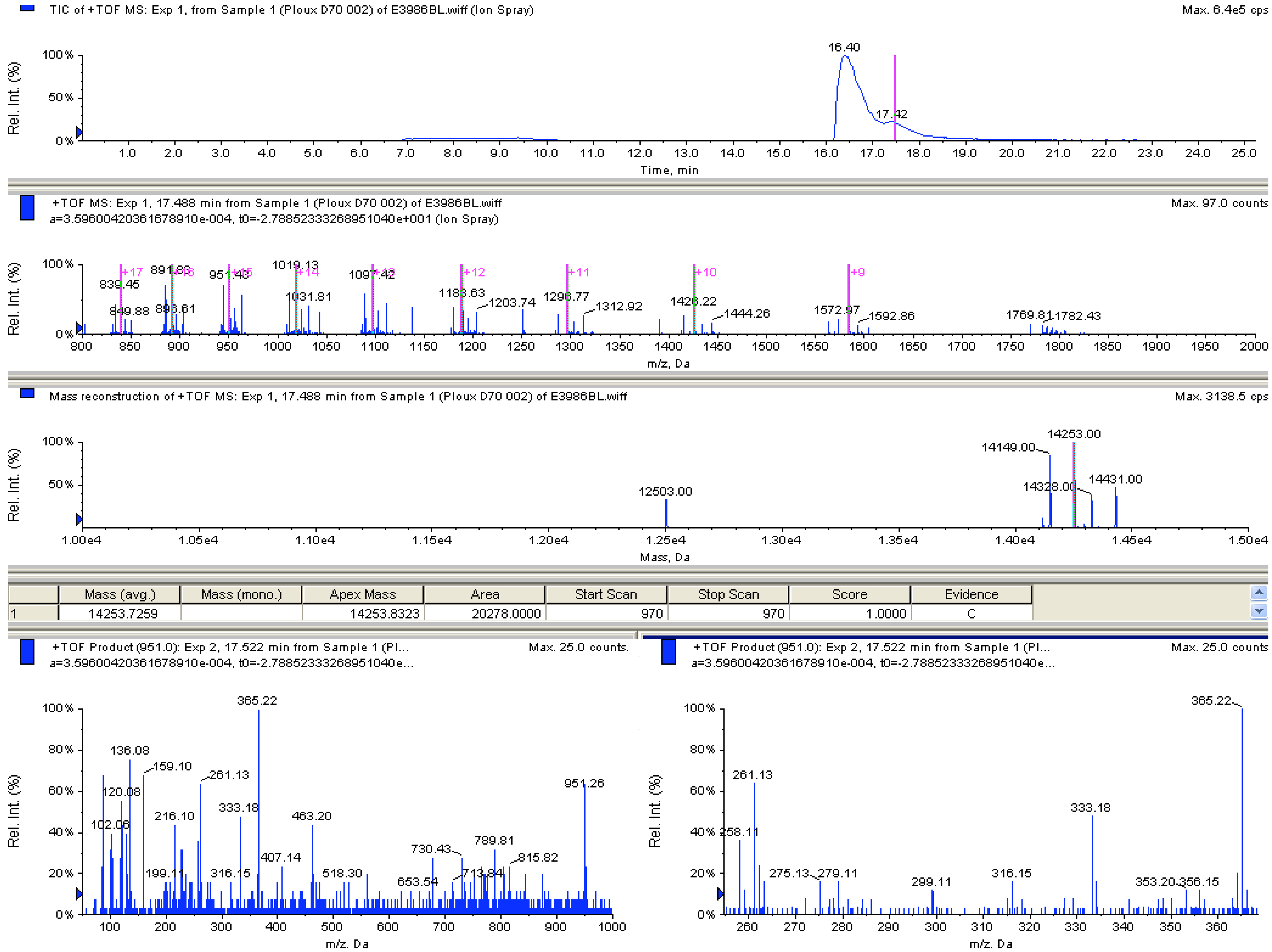
TIC of +TOF MS: Exp 1, from Sample 1 (Ploux D70 002) of E3986BL.wiff (Ion Spray)
Max. 6.4e5 cps
16.40
17.42
Time, min
+TOF MS: Exp 1, 17.488 min from Sample 1 (Ploux D70 002) of E3986BL.wiff
a=3.59600420361678910e-004, t0=-2.78852333268951040e+001 (Ion Spray)
Max. 97.0 counts
m/z, Da
Mass reconstruction of +TOF MS: Exp 1, 17.488 min from Sample 1 (Ploux D70 002) of E3986BL.wiff
Max. 3138.5 cps
14253.00
14149.00
14328.00
14431.00
12503.00
Mass, Da
Mass (avg.) | Mass (mono.) | Apex Mass | Area | Start Scan | Stop Scan | Score | Evidence
1 | 14253.7259 | | 14253.8323 | 20278.0000 | 970 | 970 | 1.0000 | C
+TOF Product (951.0): Exp 2, 17.522 min from Sample 1 (Pl...
a=3.59600420361678910e-004, t0=-2.78852333268951040e...
Max. 25.0 counts.
365.22
261.13
333.18
951.26
m/z, Da
Rel. Int. (%)

Figure S12A.

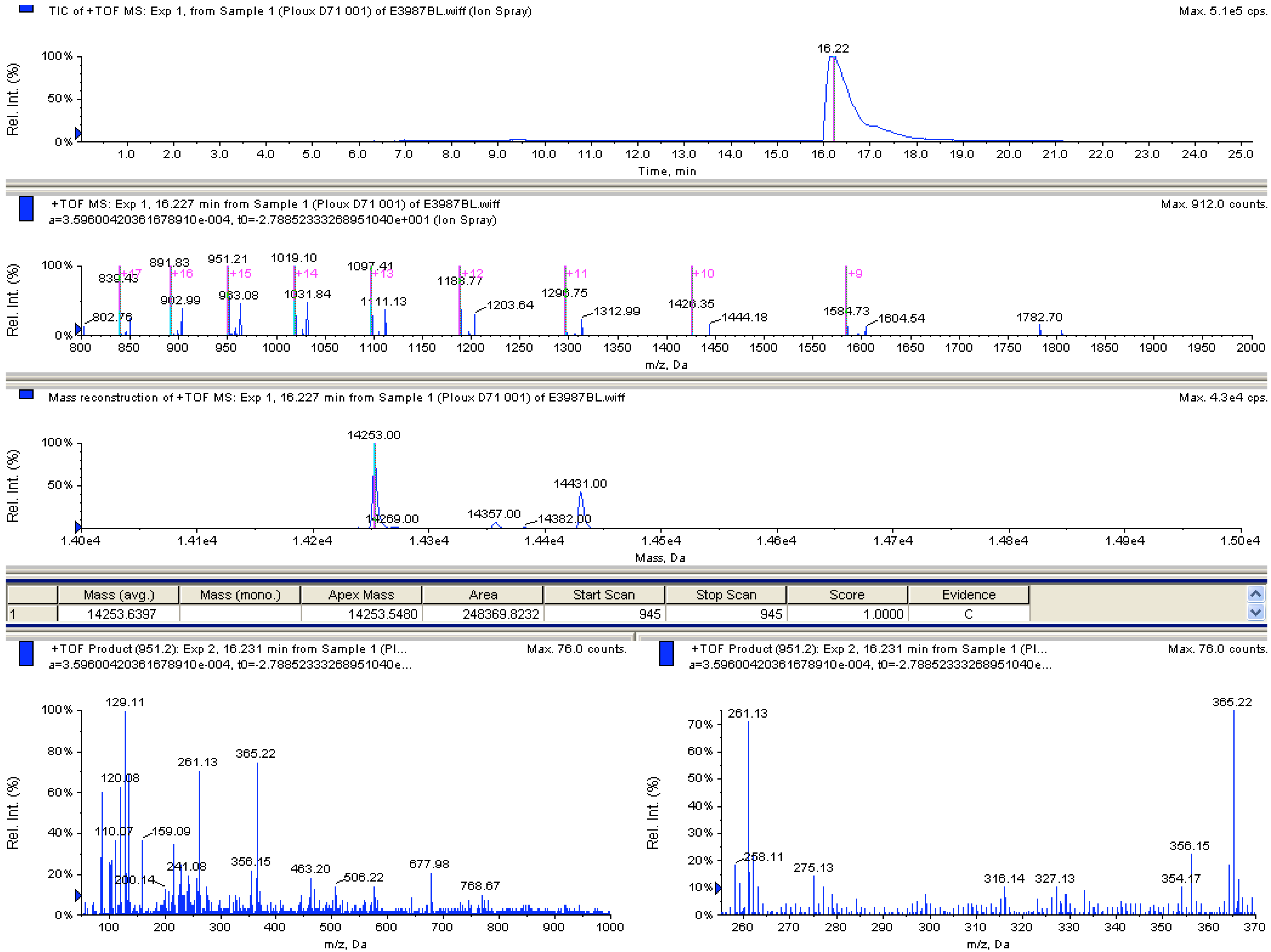

	Mass (avg.)	Mass (mono.)	Apex Mass	Area	Start Scan	Stop Scan	Score	Evidence
1	14253.6397		14253.5480	248369.8232	945	945	1.0000	C

Figure S12B.

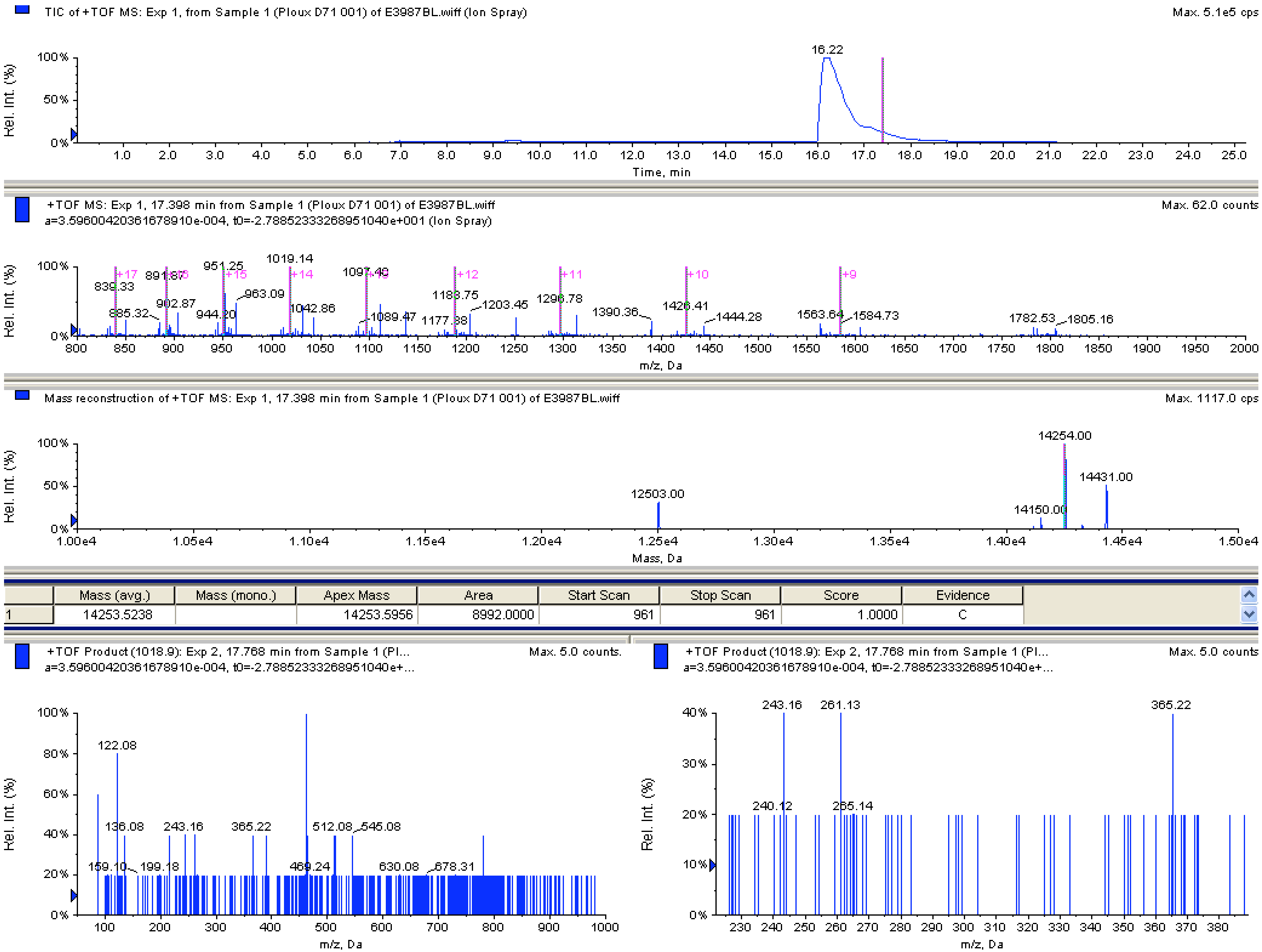
TIC of +TOF MS: Exp 1, from Sample 1 (Ploux D71 001) of E3987BL.wiff (Ion Spray)
Max. 5.1e5 cps
16.22
Rel. Int. (%)
Time, min
+TOF MS: Exp 1, 17.398 min from Sample 1 (Ploux D71 001) of E3987BL.wiff
a=3.59600420361678910e-004, t0=-2.78852333268951040e+001 (Ion Spray)
Max. 62.0 counts
839.33
885.32
891.87
902.87
944.20
951.25
963.09
1019.14
1042.86
1089.47
1097.49
1177.38
1188.75
1203.45
1296.78
1390.36
1426.41
1444.28
1563.64
1584.73
1782.53
1805.16
+17 +15 +14 +12 +11 +10 +9
m/z, Da
Mass reconstruction of +TOF MS: Exp 1, 17.398 min from Sample 1 (Ploux D71 001) of E3987BL.wiff
Max. 1117.0 cps
12503.00
14150.00
14254.00
14431.00
Mass, Da
Mass (avg.) | Mass (mono.) | Apex Mass | Area | Start Scan | Stop Scan | Score | Evidence
1 | 14253.5238 | | 14253.5956 | 8992.0000 | 961 | 961 | 1.0000 | C
+TOF Product (1018.9): Exp 2, 17.768 min from Sample 1 (Pl...
a=3.59600420361678910e-004, t0=-2.78852333268951040e+...
Max. 5.0 counts.
122.08
136.08
159.10
199.18
243.16
365.22
469.24
512.08
545.08
630.08
678.31
m/z, Da
+TOF Product (1018.9): Exp 2, 17.768 min from Sample 1 (Pl...
a=3.59600420361678910e-004, t0=-2.78852333268951040e+...
Max. 5.0 counts
240.12
243.16
261.13
265.14
365.22
m/z, Da

Figure S12C.

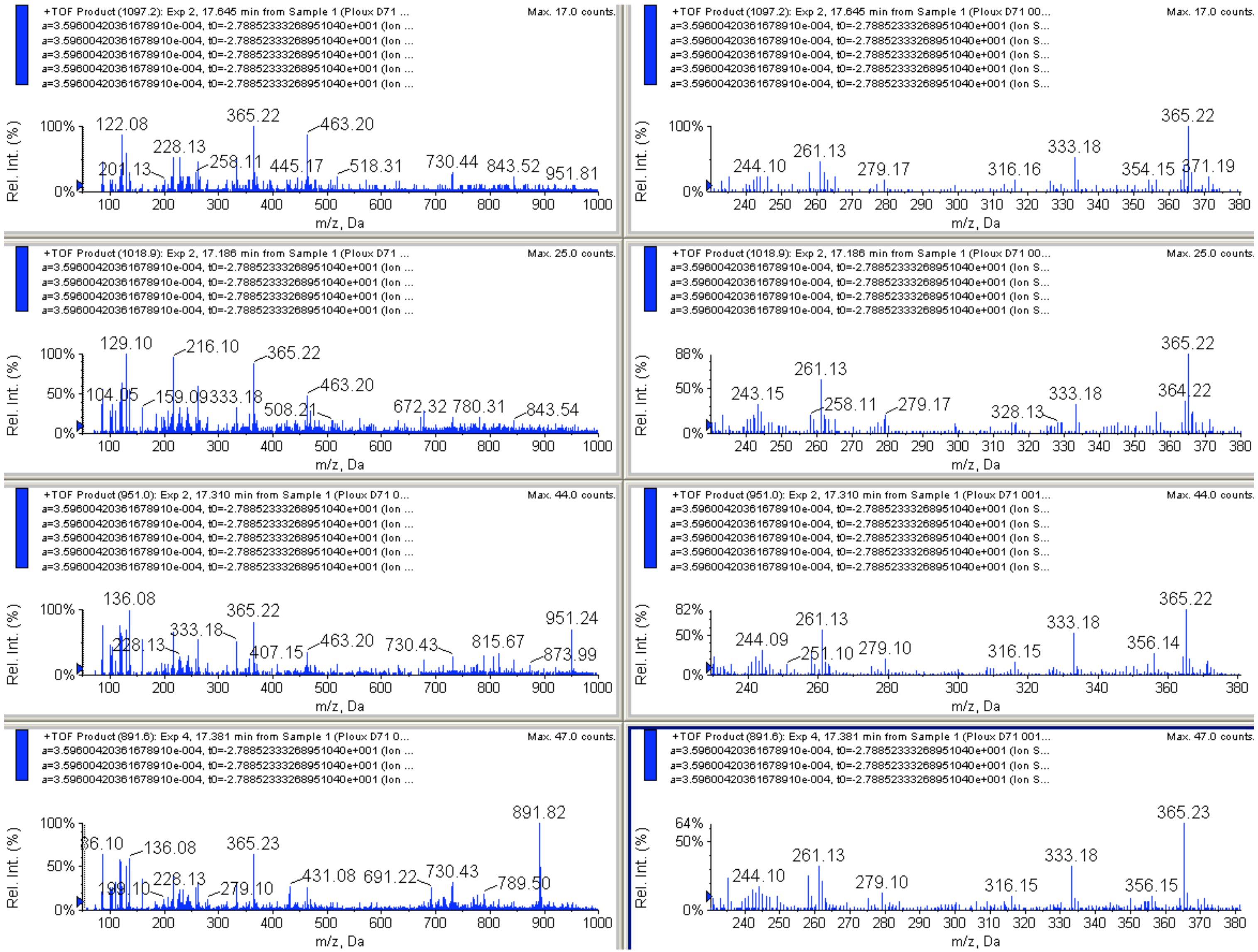
+TOF Product (1097.2): Exp 2, 17.645 min from Sample 1 (Ploux D71 ...
Max. 17.0 counts.
122.08
365.22
463.20
228.13
201.13
258.11
445.17
518.31
730.44
843.52
951.81
365.22
333.18
261.13
244.10
279.17
316.16
354.15
371.19
+TOF Product (1018.9): Exp 2, 17.186 min from Sample 1 (Ploux D71 ...
Max. 25.0 counts.
129.10
216.10
365.22
104.05
159.09
333.18
463.20
508.21
672.32
780.31
843.54
365.22
261.13
243.15
258.11
279.17
333.18
328.13
364.22
+TOF Product (951.0): Exp 2, 17.310 min from Sample 1 (Ploux D71 0...
Max. 44.0 counts.
136.08
365.22
333.18
228.13
407.15
463.20
730.43
815.67
951.24
873.99
365.22
261.13
333.18
244.09
251.10
279.10
316.15
356.14
+TOF Product (891.6): Exp 4, 17.381 min from Sample 1 (Ploux D71 0...
Max. 47.0 counts.
891.82
86.10
136.08
365.23
199.10
228.13
279.10
431.08
691.22
730.43
789.50
365.23
261.13
333.18
244.10
279.10
316.15
356.15
Rel. Int. (%)
m/z, Da

Figure S13A.

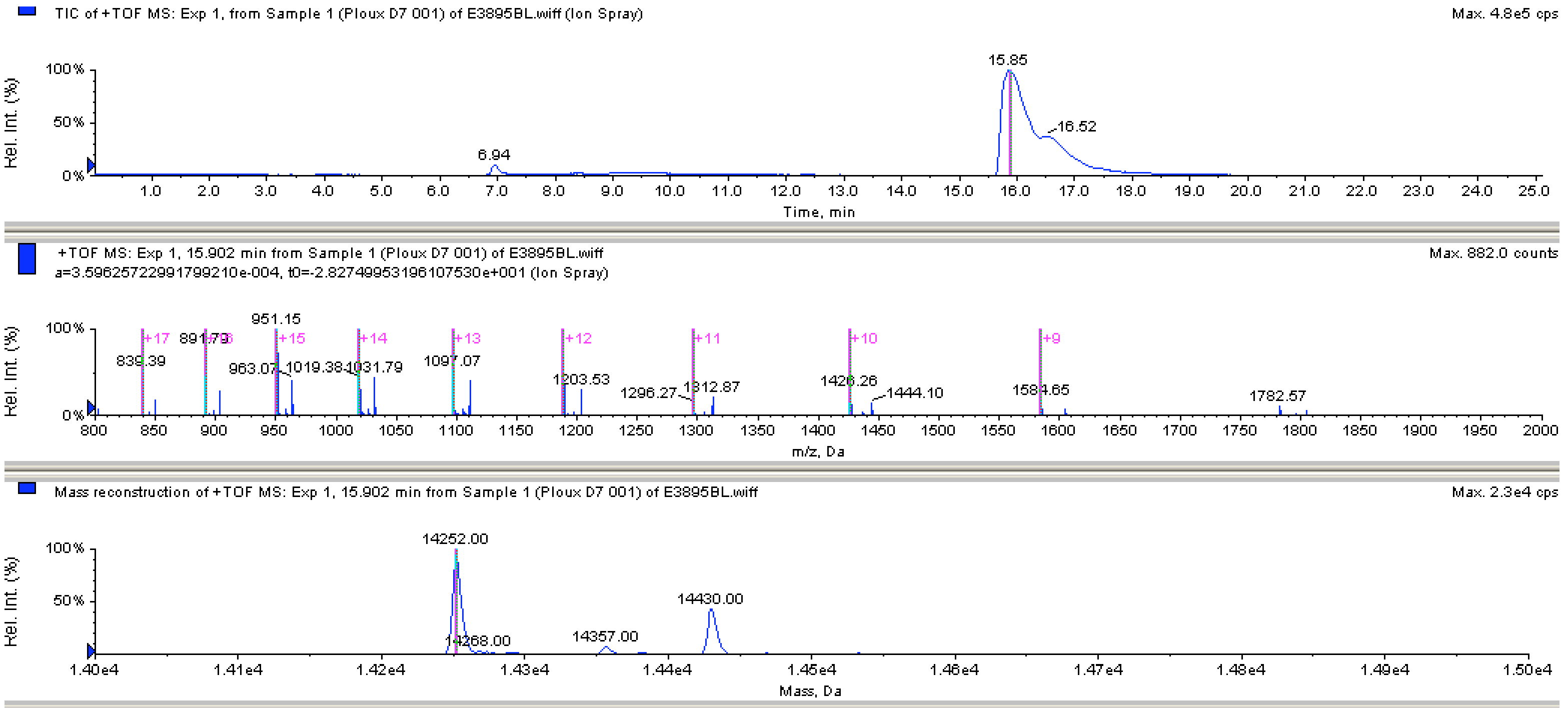

	Mass (avg.)	Mass (mono.)	Apex Mass	Area	Start Scan	Stop Scan	Score	Evidence
1	14252.4911		14252.4942	124597.0000	929	929	1.0000	C

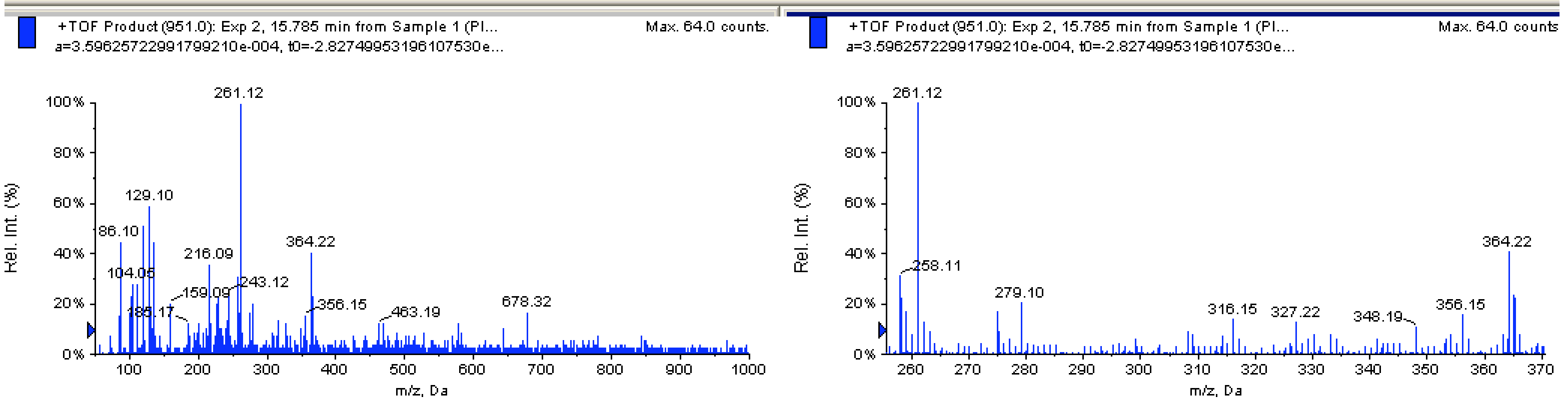

Figure S13B.

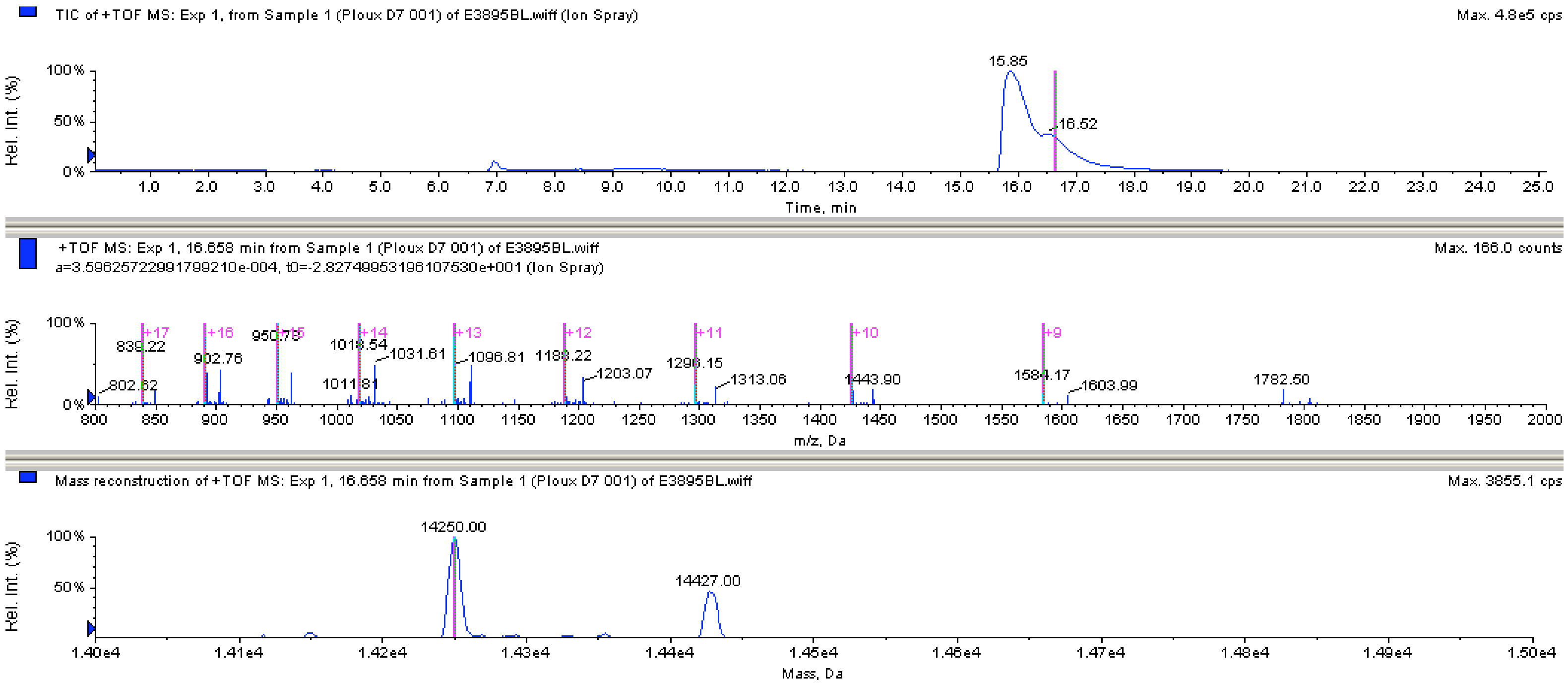

	Mass (avg.)	Mass (mono.)	Apex Mass	Area	Start Scan	Stop Scan	Score	Evidence
1	14250.0377		14250.0418	34428.0000	942	942	1.0000	C

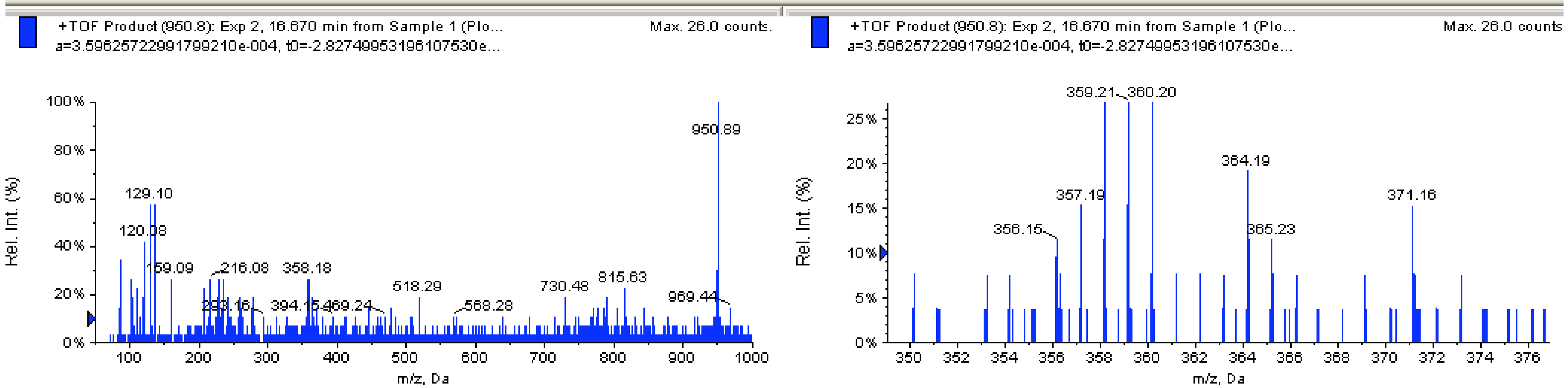

Figure S13C.

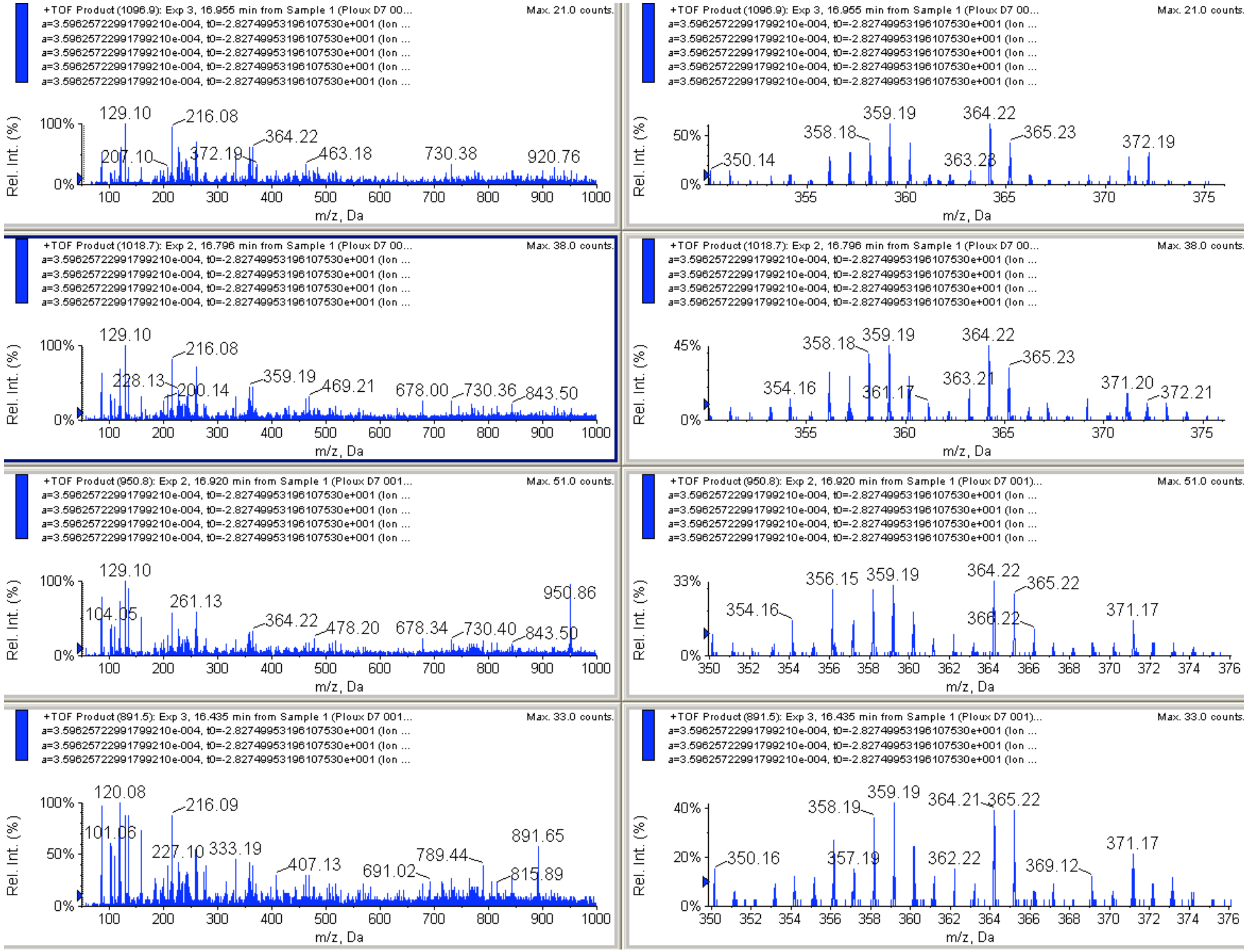
+TOF Product (1096.9): Exp 3, 16.955 min from Sample 1 (Ploux D7 00...
Max. 21.0 counts.
+TOF Product (1018.7): Exp 2, 16.796 min from Sample 1 (Ploux D7 00...
Max. 38.0 counts.
+TOF Product (950.8): Exp 2, 16.920 min from Sample 1 (Ploux D7 001...
Max. 51.0 counts.
+TOF Product (891.5): Exp 3, 16.435 min from Sample 1 (Ploux D7 001...
Max. 33.0 counts.
Rel. Int. (%)
m/z, Da

Figure S14A.

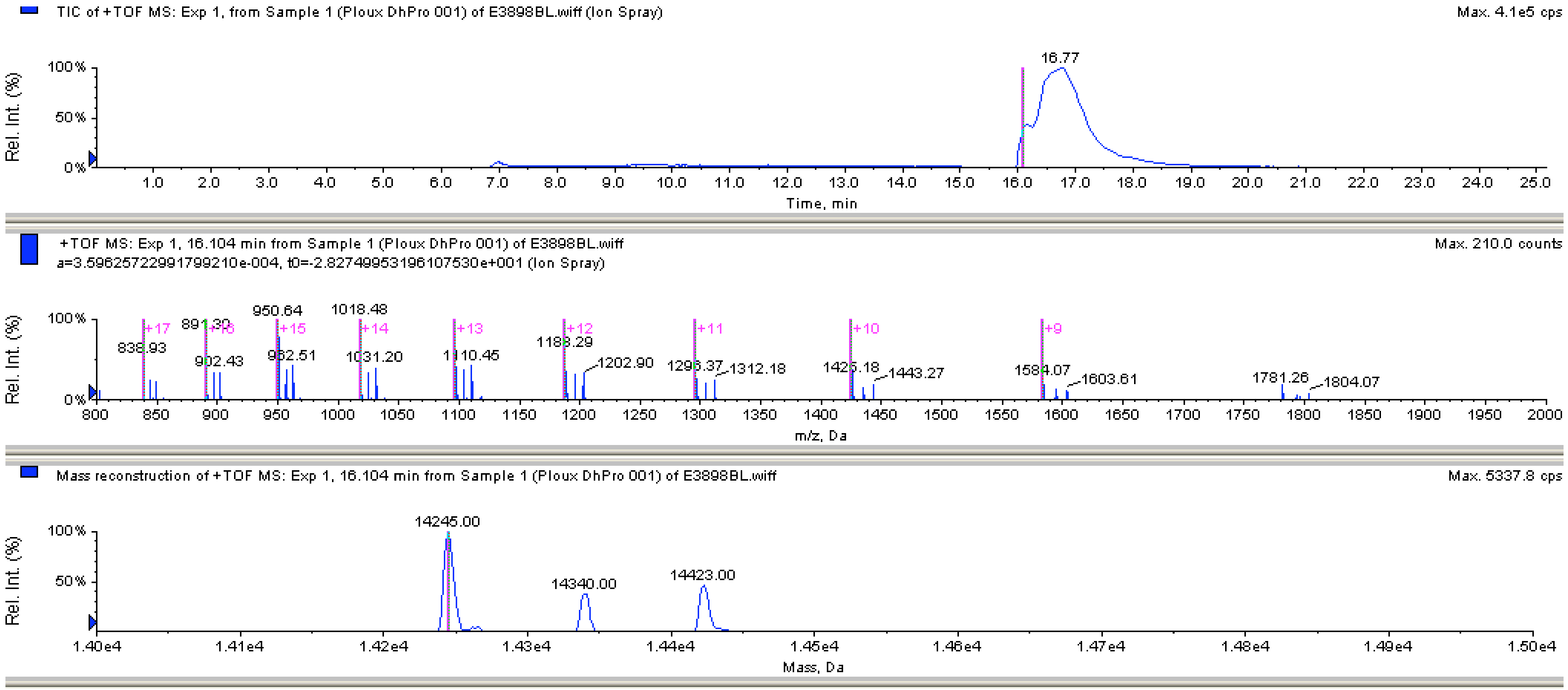

	Mass (avg.)	Mass (mono.)	Apex Mass	Area	Start Scan	Stop Scan	Score	Evidence
1	14244.7373		14244.7191	42183.0000	944	944	1.0000	C

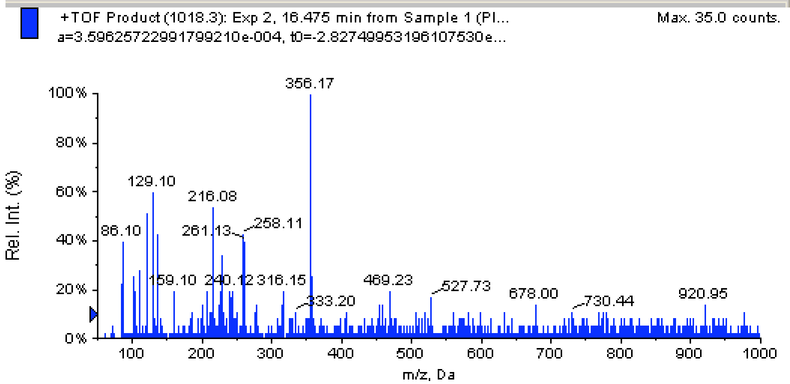

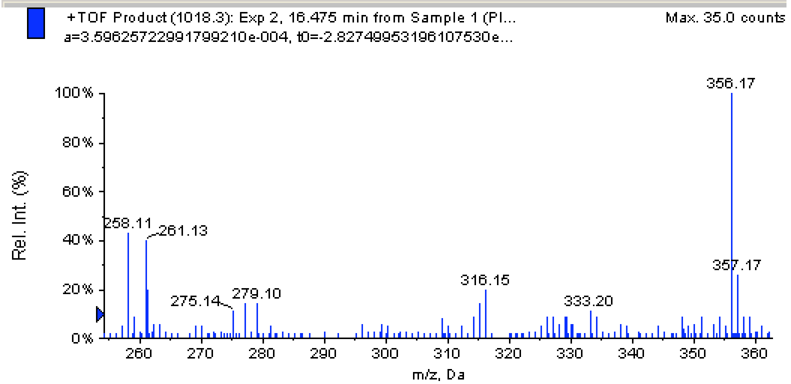

Figure S14B.

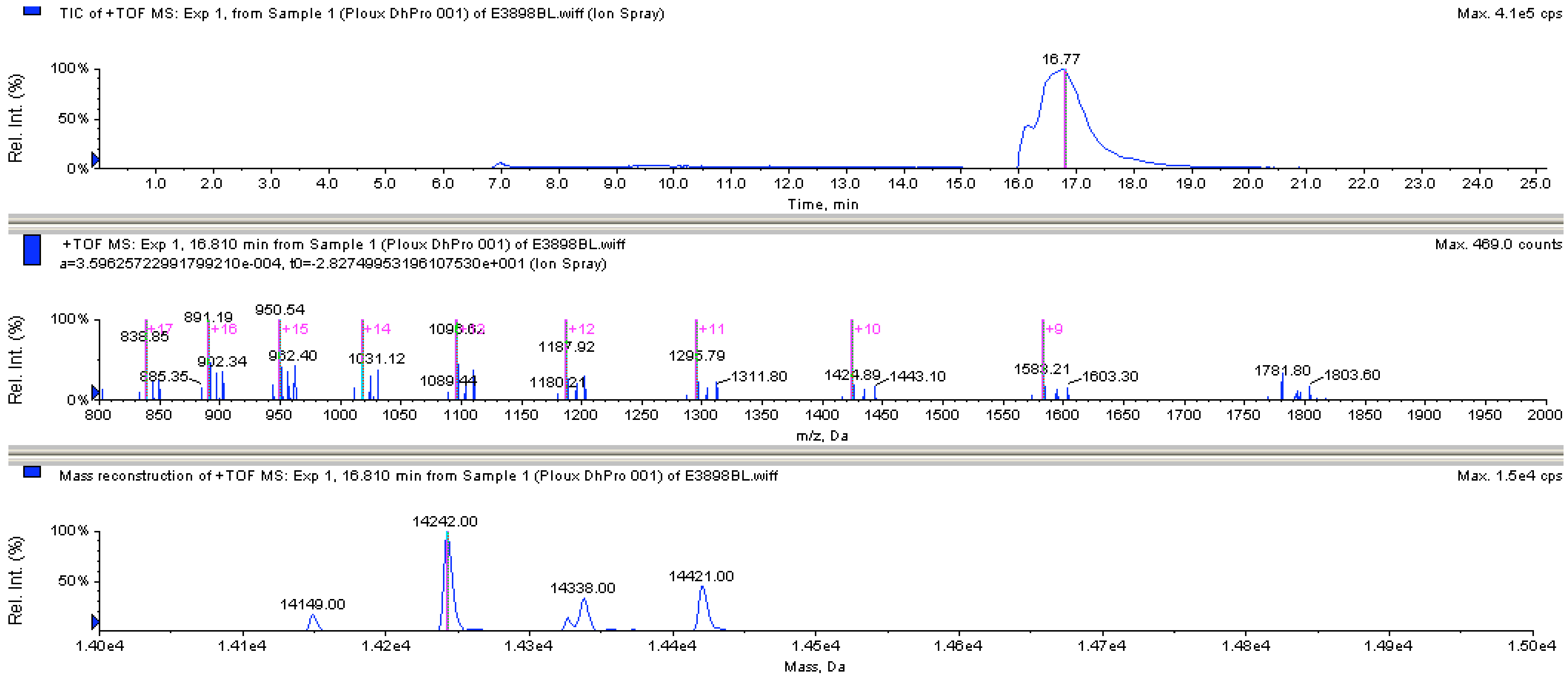

	Mass (avg.)	Mass (mono.)	Apex Mass	Area	Start Scan	Stop Scan	Score	Evidence
1	14243.0953		14243.0826	114156.0000	956	956	1.0000	C

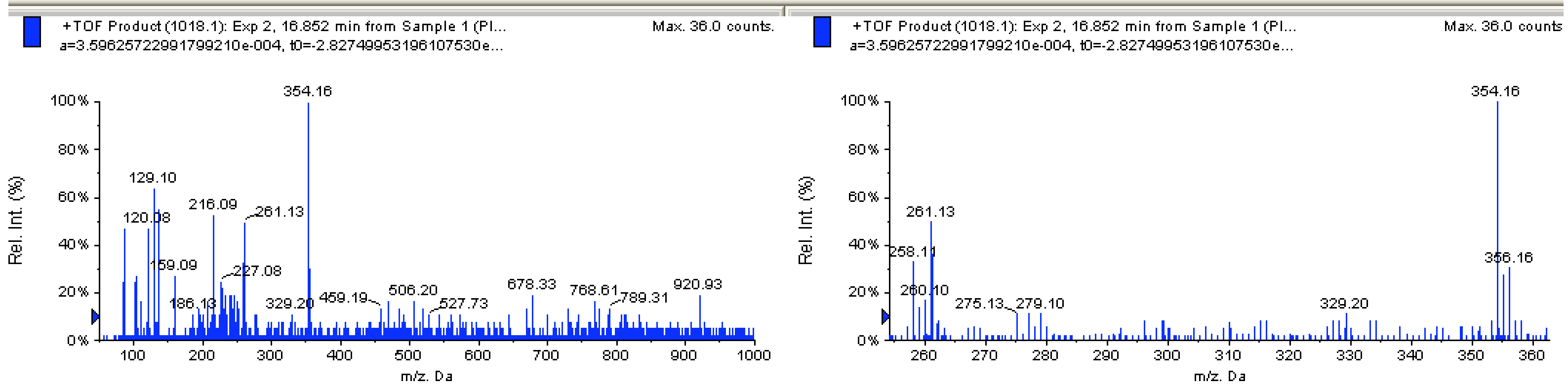

Figure S15A.

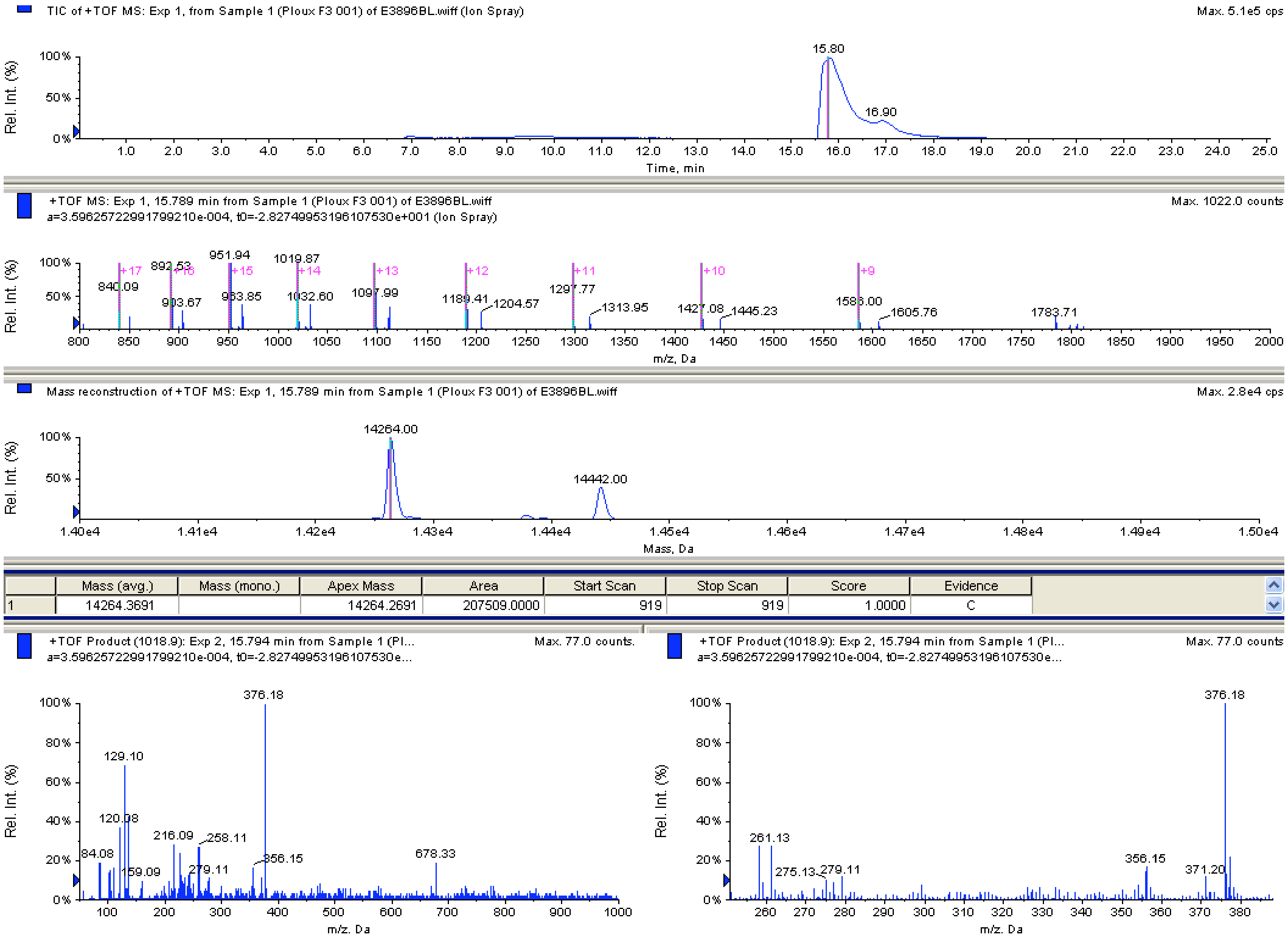
TIC of +TOF MS: Exp 1, from Sample 1 (Ploux F3 001) of E3896BL.wiff (Ion Spray)
Max. 5.1e5 cps
15.80
16.90
Rel. Int. (%)
Time, min
+TOF MS: Exp 1, 15.789 min from Sample 1 (Ploux F3 001) of E3896BL.wiff
a=3.59625722991799210e-004, t0=-2.82749953196107530e+001 (Ion Spray)
Max. 1022.0 counts
840.09
892.53
903.67
951.94
963.85
1019.87
1032.60
1097.99
1189.41
1204.57
1297.77
1313.95
1427.08
1445.23
1586.00
1605.76
1783.71
+17 +16 +15 +14 +13 +12 +11 +10 +9
m/z, Da
Mass reconstruction of +TOF MS: Exp 1, 15.789 min from Sample 1 (Ploux F3 001) of E3896BL.wiff
Max. 2.8e4 cps
14264.00
14442.00
Mass, Da
Mass (avg.) | Mass (mono.) | Apex Mass | Area | Start Scan | Stop Scan | Score | Evidence
1 | 14264.3691 | | 14264.2691 | 207509.0000 | 919 | 919 | 1.0000 | C
+TOF Product (1018.9): Exp 2, 15.794 min from Sample 1 (Pl...
a=3.59625722991799210e-004, t0=-2.82749953196107530e...
Max. 77.0 counts.
376.18
129.10
120.08
84.08
216.09
258.11
159.09
279.11
356.15
678.33
m/z, Da
+TOF Product (1018.9): Exp 2, 15.794 min from Sample 1 (Pl...
a=3.59625722991799210e-004, t0=-2.82749953196107530e...
Max. 77.0 counts
376.18
261.13
275.13
279.11
356.15
371.20
m/z, Da

Figure S15B.

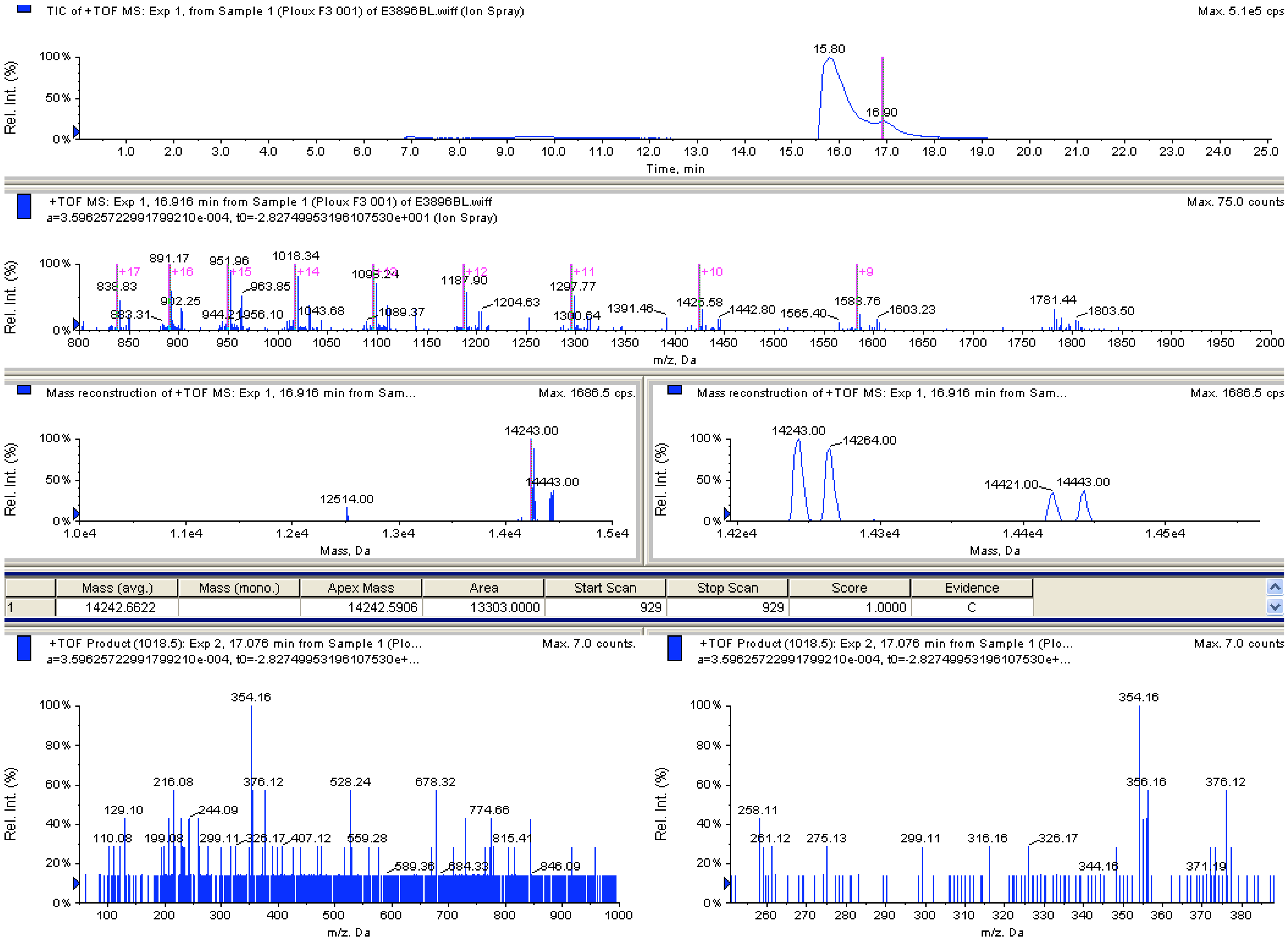
TIC of +TOF MS: Exp 1, from Sample 1 (Ploux F3 001) of E3896BL.wiff (Ion Spray)
Max. 5.1e5 cps
15.80
16.90
Time, min
Rel. Int. (%)
+TOF MS: Exp 1, 16.916 min from Sample 1 (Ploux F3 001) of E3896BL.wiff
a=3.59625722991799210e-004, t0=-2.82749953196107530e+001 (Ion Spray)
Max. 75.0 counts
891.17
951.96
1018.34
838.83
902.25
883.31
963.85
944.21
956.10
1043.68
1089.37
1187.90
1204.63
1297.77
1300.64
1391.46
1442.80
1565.40
1603.23
1781.44
1803.50
+17
+16
+15
+14
+12
+11
+10
+9
m/z, Da
Mass reconstruction of +TOF MS: Exp 1, 16.916 min from Sam...
Max. 1686.5 cps.
14243.00
14443.00
12514.00
14264.00
14421.00
Mass, Da
Mass (avg.) | Mass (mono.) | Apex Mass | Area | Start Scan | Stop Scan | Score | Evidence
1 | 14242.6622 | | 14242.5906 | 13303.0000 | 929 | 929 | 1.0000 | C
+TOF Product (1018.5): Exp 2, 17.076 min from Sample 1 (Plo...
a=3.59625722991799210e-004, t0=-2.82749953196107530e+...
Max. 7.0 counts
354.16
216.08
376.12
528.24
678.32
129.10
244.09
774.66
110.08
199.08
299.11
326.17
407.12
559.28
815.41
589.36
684.33
846.09
258.11
261.12
275.13
316.16
344.16
356.16
371.19
m/z, Da

Figure S15C.

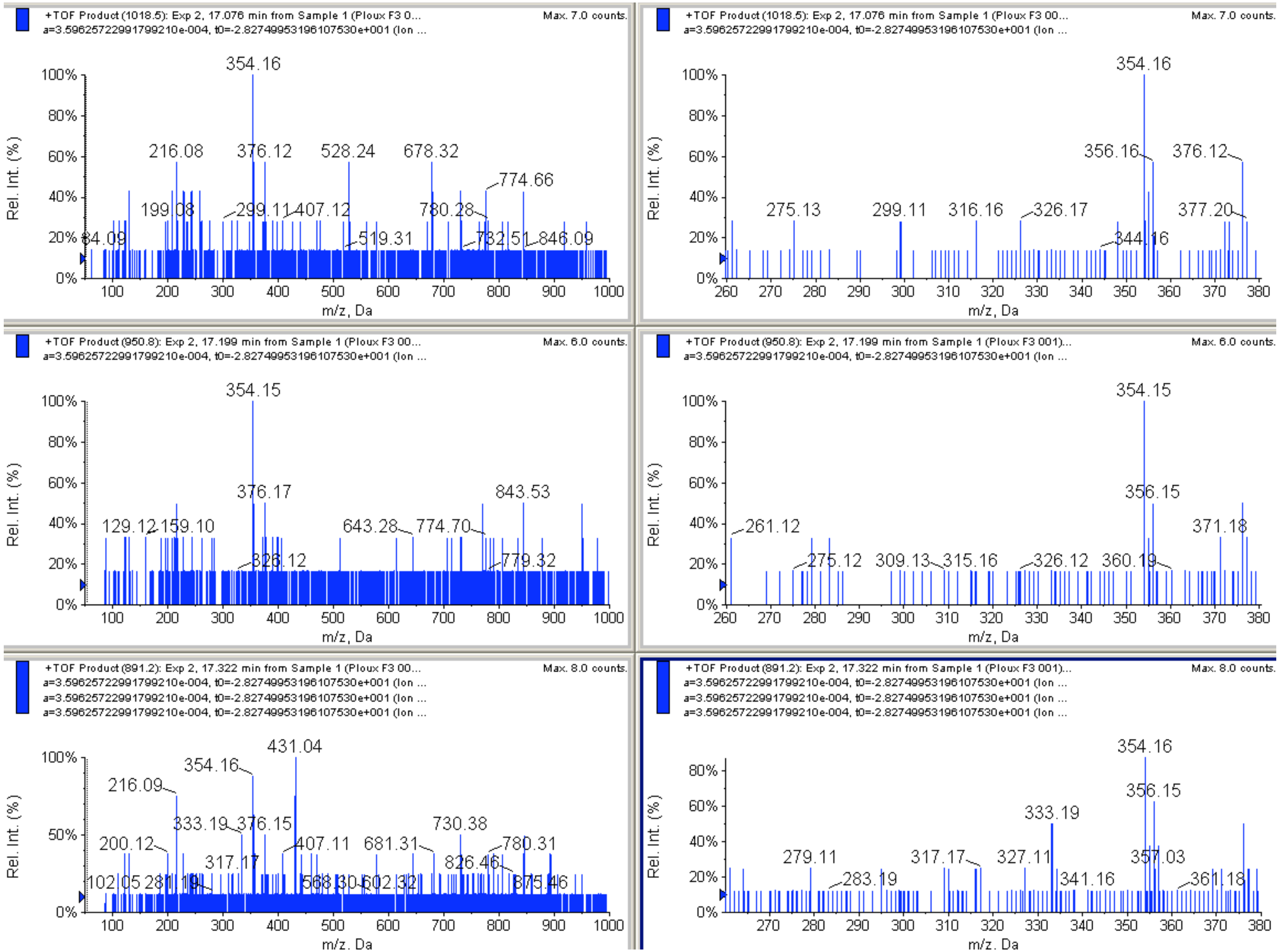

Figure S16A.

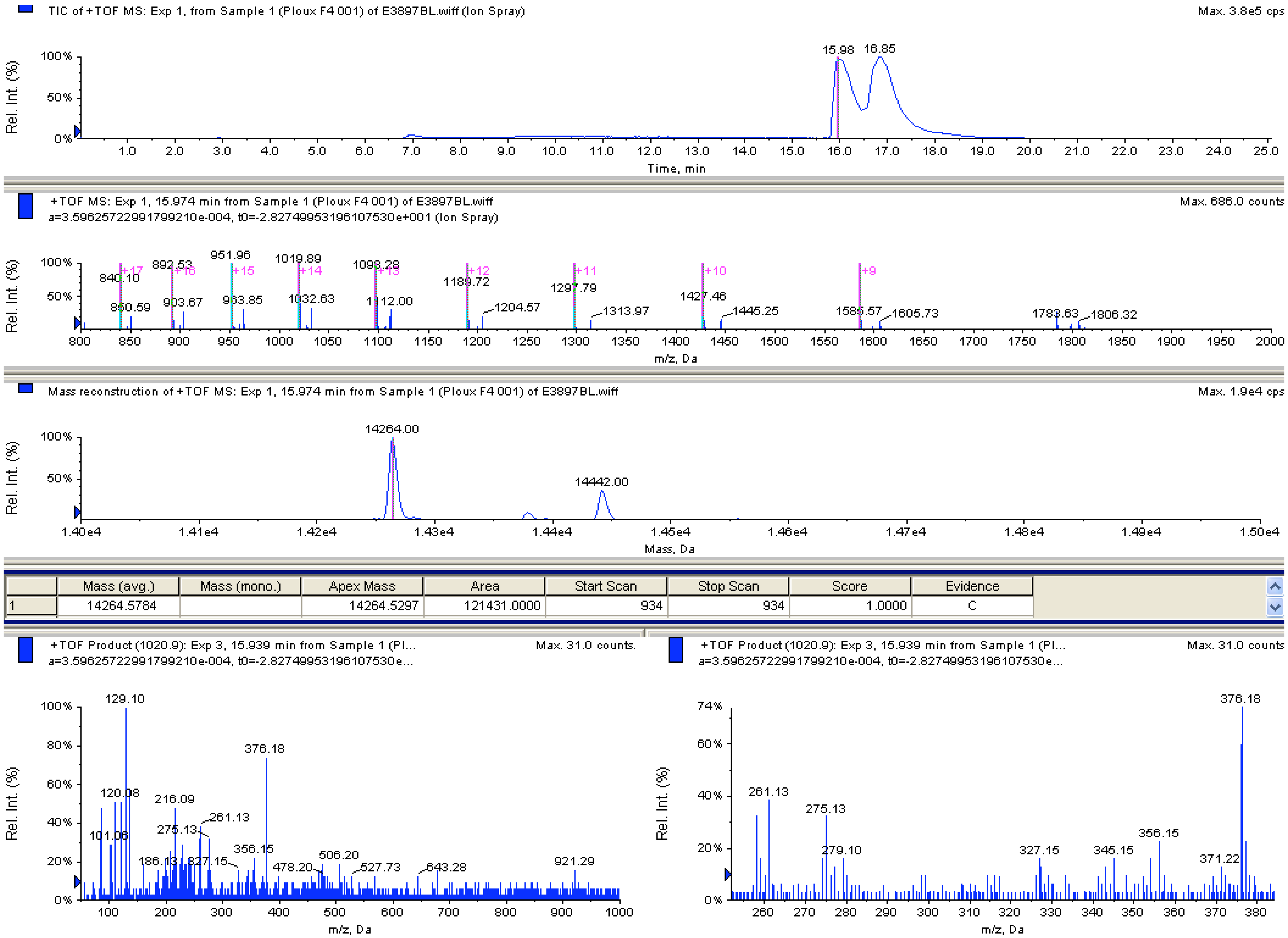
TIC of +TOF MS: Exp 1, from Sample 1 (Ploux F4 001) of E3897BL.wiff (Ion Spray)
Max. 3.8e5 cps
15.98
16.85
Time, min
+TOF MS: Exp 1, 15.974 min from Sample 1 (Ploux F4 001) of E3897BL.wiff
a=3.59625722991799210e-004, t0=-2.82749953196107530e+001 (Ion Spray)
Max. 686.0 counts
m/z, Da
Mass reconstruction of +TOF MS: Exp 1, 15.974 min from Sample 1 (Ploux F4 001) of E3897BL.wiff
Max. 1.9e4 cps
14264.00
14442.00
Mass, Da
Mass (avg.) | Mass (mono.) | Apex Mass | Area | Start Scan | Stop Scan | Score | Evidence
1 | 14264.5784 | | 14264.5297 | 121431.0000 | 934 | 934 | 1.0000 | C
+TOF Product (1020.9): Exp 3, 15.939 min from Sample 1 (Pl...
a=3.59625722991799210e-004, t0=-2.82749953196107530e...
Max. 31.0 counts.
129.10
376.18
m/z, Da
Rel. Int. (%)

Figure S16B.

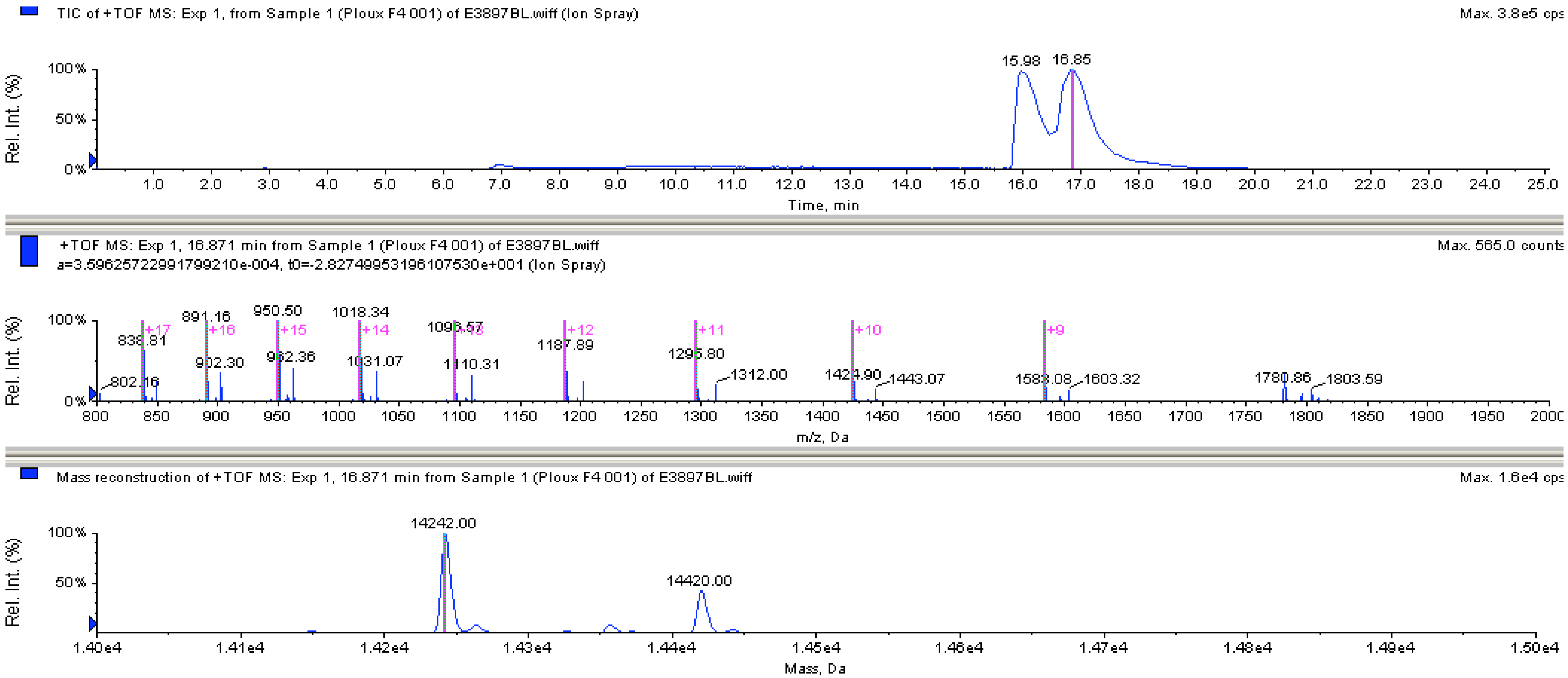

	Mass (avg.)	Mass (mono.)	Apex Mass	Area	Start Scan	Stop Scan	Score	Evidence
1	14242.5209		14242.4737	74977.0000	943	943	1.0000	C

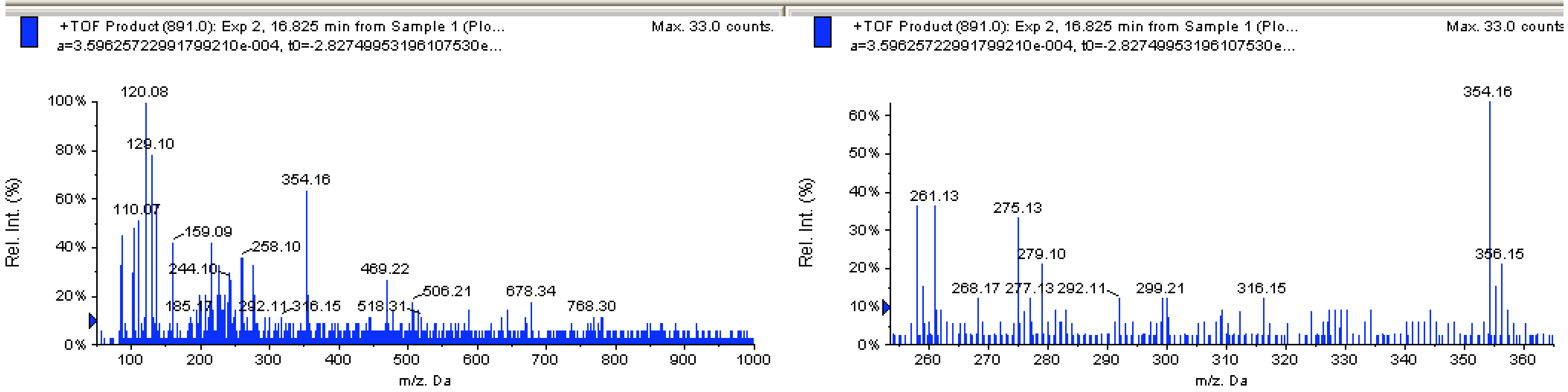

Figure S17. The isotopic distributions of ions arising from labeled prolyl-AnaDs were simulated by first calculating the relative abundance of the different species (containing zero, one, two, and more deuterium) and then by calculating for each species its isotopic distribution at unitary resolution. The relative abundance of the species of the same apparent mass (M, M+1, M+2, M+i, i for integer) were then summed and plotted, after normalization. The deuterium labeling of the ions arising from [5,5-$^{2}H_{2}$]-L-prolyl-AnaD and from [2,3,3,4,4,5,5-$^{2}H_{7}$]-L-prolyl-AnaD was considered randomly distributed on two or seven positions, respectively. The isotopic distributions of the ions ejected from the products were predicted by considering a complete loss of deuterium at position C2, and either a non-stereospecific exchange on C5 positions or a stereospecific or non-stereospecific loss at C5 positions or, and a non-stereospecific exchange on positions C3 and C4. The plots corresponding to the oxidation of the C5-labeled substrates are shown in Figure 4 of the main text. Detailed calculations are given at the end of this Figure.

Ion from [2-^{2}H]-L-prolyl-AnaD

cacld	obsd
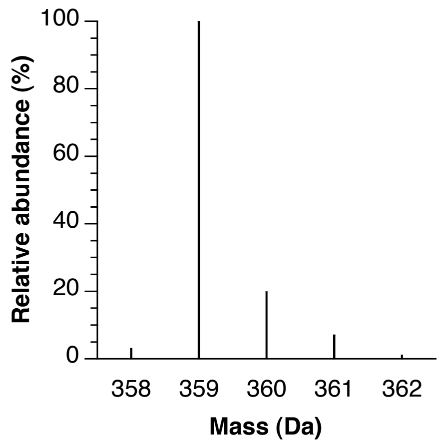	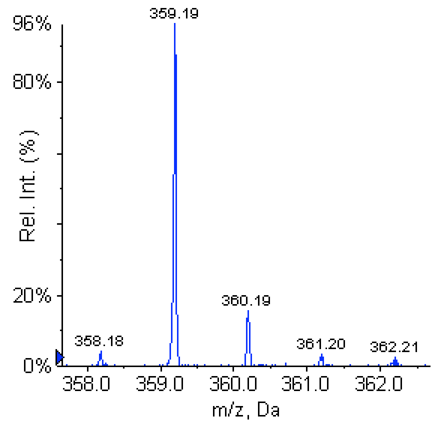

Ion from [5,5-$^{2}H_{2}$]-L-prolyl-AnaD

cacld	obsd
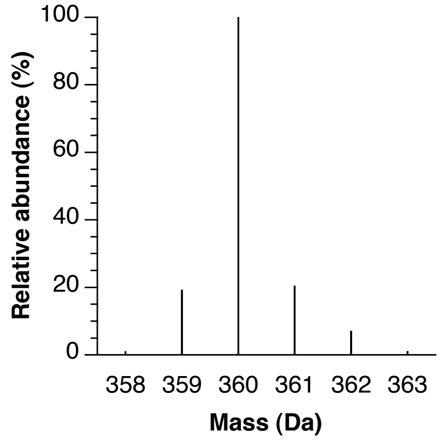	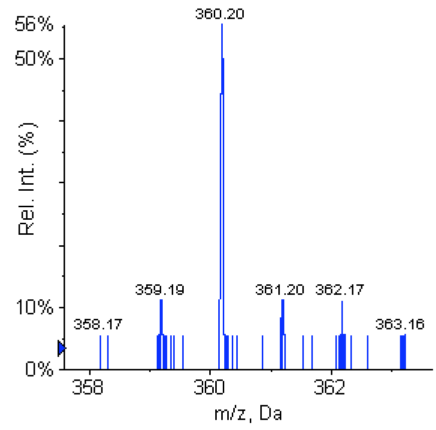

Ion from (5*S*)-[5-^{2}H]-L-prolyl-AnaD

cacld

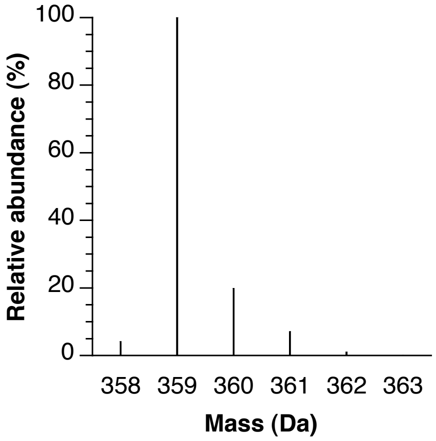

obsd

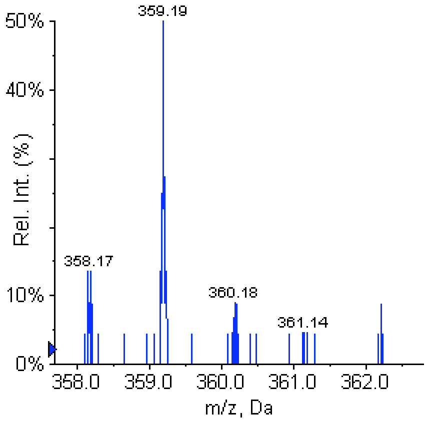

Ion from [2,3,3,4,4,5,5-$^{2}H_{7}$]-L-prolyl-AnaD

cacld

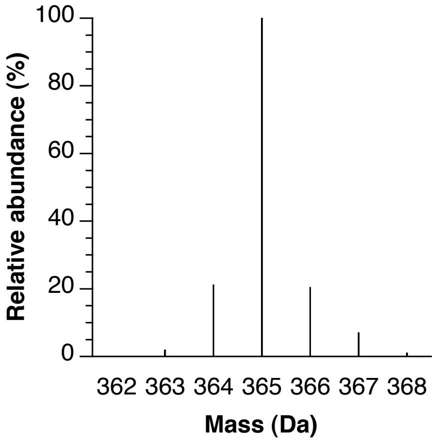

obsd

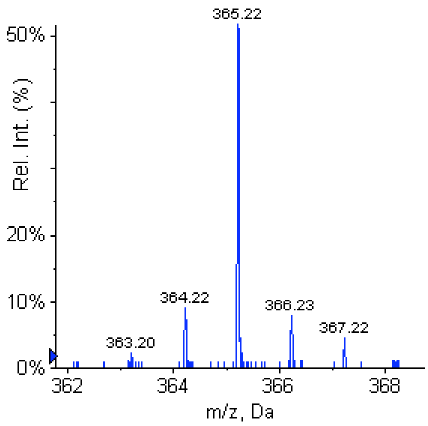

Predicted and observed isotopic distribution for the ion arising from the oxidation product of [2-^{2}H]-L-prolyl-AnaD.

cacld

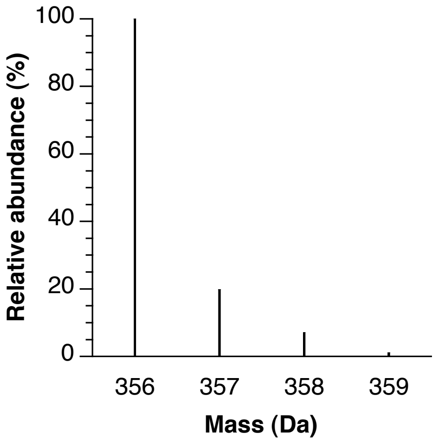

obsd

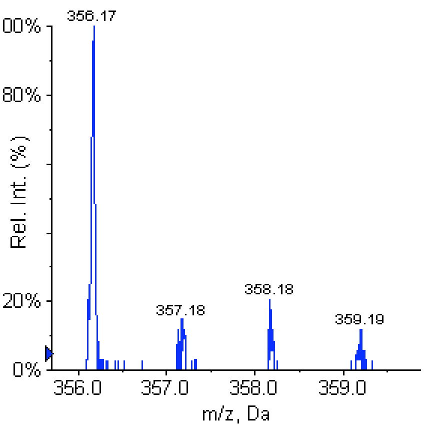

Predicted and observed isotopic distribution for the ion arising from the oxidation product of [2,3,3,4,4,5,5-$^{2}H_{7}$]-L-prolyl-AnaD.

cacld	obsd
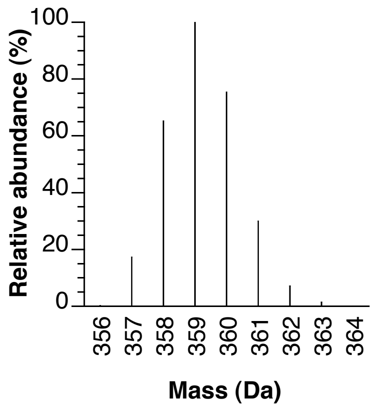	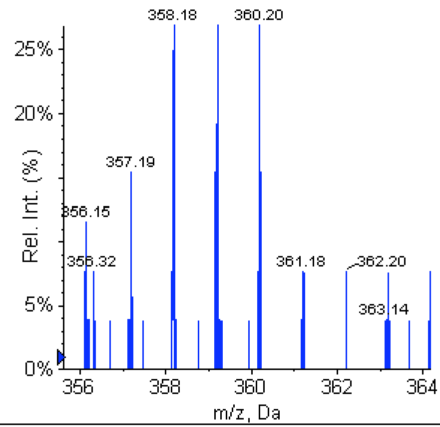

Method used to simulate the isotopic distributions for substrates and products.

The natural isotopic abundance up to M+3, used for all the ions is indicated below. Since all ions only differ in the number of hydrogen or deuterium, the relative abundance will be the same and is given for the molecular formula $C_{16}H_{28}O_{4}N_{3}S$ (ion ejected from prolyl-AnaD).

Mass		**Normalized relative abundance (%)**	**Fractional relative abundance**
358	M	100.0	0.78
359	M+1	19.8	0.16
360	M+2	7.1	0.05
361	M+3	1.1	0.01

For any species Mi of mass M and relative abundance a, and for its isotopologues Mi+1, of mass M+1 and relative abundance b, Mi+2 of mass M+2 and relative abundance c, etc., the isotopic distribution will be as follows:

Mi	**Mi+1**	**Mi+2**	**Fractional relative abundance**	**Mass**
0.78 × a			0.78 × a	M
0.16 × a	0.78 × b		0.16 × a + 0.78 × b	M+1
0.05 × a	0.16 × b	0.78 × c	0.05 × a + 0.16 × b + 0.78 × c	M+2
0.01 × a	0.05 × b	0.16 × c	0.01 × a + 0.05 × b + 0.16 × c	M+3
	0.01 × b	0.05 × c	0.01 × b + 0.05 × c	M+4
		0.01 × c	0.01 × c	M+5

This distribution can then be normalized by setting the relative abundance of the most abundant species at 100.0%. The isotopic distribution of the substrates was thus calculated using the following relative abundance for the deuterated species:

[2-^{2}H]-L-prolyl-AnaD is composed of 3% D_0 (M) and 97% D_1 (M+1) species.

[5,5-$^2H_2$]-L-prolyl-AnaD is composed of ($0.09^2 = 0.0081$) 0.81% D_0 (M), ($2 \times 0.09 \times 0.91 = 0.164$) 16.4% D_1 (M+1), and ($0.97^2 = 0.828$) 82.8% D_2 (M+2) species.

(5*S*)-[5-^{2}H]-L-prolyl-AnaD is composed of 4% D_0 (M), 14% of (5*R*)-derivative and 82% of (5*S*)-derivative, both D_1 species (M+1).

[2,3,3,4,4,5,5-$^2H_7$]-L-prolyl-AnaD is composed of D_0 (M) to D_7 (M+7) species which relative abundances are given below. We only considered the D_4 to D_7 species for the calculation of the isotopic distribution of the substrate.

Species		Fraction	Relative abundance (%)
D_0	M	0.03^7	-
D_1	M+1	$7 \times 0.97 \times 0.03^6$	-
D_2	M+2	$21 \times 0.97^2 \times 0.03^5$	-
D_3	M+3	$35 \times 0.97^3 \times 0.03^4$	-
D_4	M+4	$35 \times 0.97^4 \times 0.03^3$	0.08%
D_5	M+5	$21 \times 0.97^5 \times 0.03^2$	1.6%
D_6	M+6	$7 \times 0.97^6 \times 0.03$	17.5%
D_7	M+7	0.97^7	80.8%

The isotopic distribution of the products was calculated by considering a complete loss of deuterium at position C2. Thus, the isotopic distribution for the ion ejected from the oxidized product of [2-^{2}H]-L-prolyl-AnaD is the natural isotopic distribution for the ion of *m/z* 356. For the oxidation of the substrates labeled on position C5, we considered two limiting cases. The first one involves a non-stereospecific loss of labeling by exchange of 50% of the deuterium with proton at both C5 positions of the P2C-AnaD intermediate. There are thus, in this case, two independent exchanges with a probability of 0.5 for each. In the other limiting case, we considered a complete loss of the labeling, either by complete exchange or by transformation of P2C-AnaD to P5C-AnaD. This loss could be stereospecific or non-stereospecific. The calculations are illustrated below.

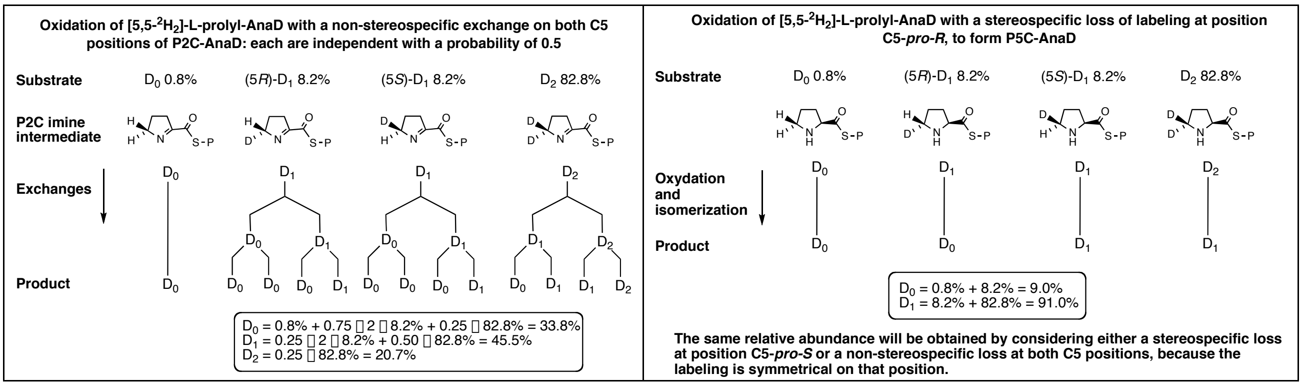

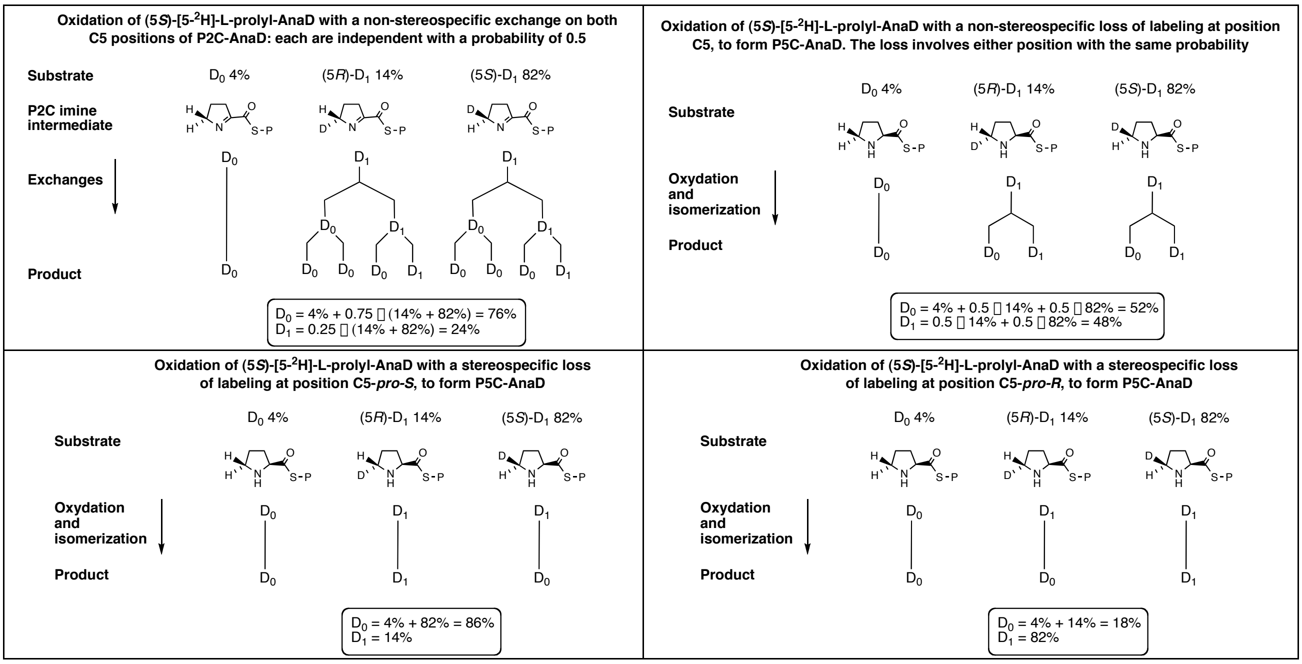

For simulating the isotopic distribution for the ion ejected from the oxidized product of [2,3,3,4,4,5,5-$^2H_7$]-L-prolyl-AnaD, we considered a complete loss of deuterium at position C2 and C5-*pro-R*, and a non-stereospecific loss at positions C3 and C4. We only considered the D_4 and D_5 imine products because the other isotopologues (D_0 to D_3) are negligible in quantity. Thus, the calculated relative abundance of these two imines are: $0.97^5 = 0.859$ (85.9%) for the D_5 species, and $5 \times (0.97)^4 \times 0.03 = 0.133$ (13.3%) for the D_4 species. There are five D_4 isotopomers depending on the position of the hydrogen. The isotopomer with one hydrogen on position C5 will have the same exchange pattern than that of the D_5 isotopomer. The four other D_4 isotopomers will give the same pattern. Considering independent exchanges on four positions with a probability of 0.5 for each exchange, the relative abundances of the exchanged species are the followings:

Imines				**Exchanged imines**	
D_5 (c)		D_4 C5-H (b)	D_4 C5-D (4 × b)		
c = 0.859		b = 0.027	4 × b = 0.106		
D_5	1/16 × c	0	0	1/16 × c	5.4% D_5
D_4	4/16 × c	1/16 × b	2/16 × 4 × b	4/16 × c + 9/16 × b	23.0% D_4
D_3	6/16 × c	4/16 × b	6/16 × 4 × b	6/16 × c + 28/16 × b	36.9% D_3
D_2	4/16 × c	6/16 × b	6/16 × 4 × b	4/16 × c + 30/16 × b	26.5% D_2
D_1	1/16 × c	4/16 × b	2/16 × 4 × b	1/16 × c + 12/16 × b	7.4% D_1
D_0	0	1/16 × b	0	1/16 × b	0.2% D_0

Non-stereospecific loss of labeling at positions C3 and C4 in the oxidized product of [$^{2}H_{7}$]-L-prolyl-AnaD, by considering independent exchanges, each with a probability of 0.5